Internship Automotive Technology

AUTOMOTIVE SHOCK ABSORBER CHARACTERISATION
USING A HYDRAULIC RIG

DC 2017.008

Supervisor TU/e:
Prof.Dr. H. Nijmeijer (Henk) h.nijmeijer@tue.nl

Ford LPG Mentor:
R. Hendrikx (Roy) rhendri9@ford.com

Author:
T. de Morée (Tim) t.d.moree@student.tue.nl
0944052

MSc. Automotive Technology
Specialisation Dynamics & Control

Eindhoven University of Technology

January 17, 2017

Preface

The purpose of this report is to document all findings during my three month internship at the Lommel Proving Ground of Ford Motor Company. The main subject of this internship was to enhance the current damper test method. This method needed to be updated to conform the updated damper test rig. A complete, easy to use post-processing tool had to be developed to be able to quickly report a damper test. Next to this, the rig was tuned to get a good performance for standard damper testing. This internship position was given out by the Advanced driving attributes Methods and Tools (AMT) group within the Research and Advanced Engineering group of Ford Motor Company.

The Ford Lommel Proving Ground (LPG) was founded in 1965. As part of the product development organisation within Ford Europe, it provides a comprehensive suite of world class vehicle test and development facilities. The main activities at LPG are part of Ford's product verification and testing and include a broad spectrum of road tests. The data recorded during these tests is analysed and processed at LPG and afterwards reported to the development centres.

Acknowledgements

This internship could not even have taken place without the help of Prof. Dr. Nijmeijer, Dr. Ir. Besselink and Prof. Dr. Ir. Zegelaar. I would like to thank them for their support in arranging an internship position at Ford Lommel Proving Ground. Next, I would also like to thank David Longin and Roy Hendrikx for giving me the opportunity to do my internship in their team. I would like to thank Roy Hendrikx in particular for being my mentor throughout this three month internship.

I would also like to thank the NVH department for their help with the damper test rig and being supportive for my questions. And I would like to thank development engineer Bart Dekoninck for his feedback on my report and his insights into shock absorber tuning.

To conclude my acknowledgements, I would like to thank Postdoc Researcher Tom van der Sande for his elaborate feedback and insights on this report which greatly improved the quality of this work.

Abstract

Ride comfort is an important aspect each time a newly developed car is launched. To cope with external vibrations, the spring-damper combination in the suspension system of a car should be properly designed. The hydraulic damper, commonly known as the shock absorber, is a key part of the suspension system as it dissipates the energy of the shocks and vibrations. This energy is dissipated through friction. There are three types of friction in a shock absorber: dry solid friction, fluid viscous friction and fluid dynamic friction.

There are two main classifications of automotive shock absorbers: monotube and twintube. Both feature a working chamber filled with a liquid (usually oil) through which a piston and rod assembly is moved to generate a damping force. They also contain a gas (usually oxygen or nitrogen) to avoid cavitation and to be able to cope with rod insertion. These types of shock absorbers can be tuned to get an optimal trade-off in performance (safety) versus comfort. Comfort in this report is defined in relation to the ISO 2631-1 standard. Tuning can be done by changing the valve characteristics around the piston of the shock absorber. The valve properties are created by a stack of discs with a certain stiffness and lay-out of holes.

After a shock absorber has been tuned, one can characterise it on a shock absorber rig (SAR). The Lommel Proving Ground (LPG) has a servo-hydraulic SAR. This SAR can be configured to perform a multitude of tests contained in a measurement procedure. The characterisation measurement procedure established during this internship consists of a lock check, temperature check, friction and gas test, and a VDA standard + high speed test. During the lock check, the SAR checks if the shock absorber is positioned correctly to ensure safe operation and avoid damage to the shock absorber and the rig. The temperature check is added to make sure the shock absorber has an appropriate starting temperature. The performance of the shock absorber is influenced by temperature. The friction and gas test is the first characterisation test. During the test the shock absorber is compressed and extended with an amplitude of 10 mm with a delay between the strokes. The test is performed at a very low stroke velocity of 0.4 mm/s to eliminate the damping force generation by the oil. As a result of the test, the gas force, static friction at extension/compression and the sliding friction are obtained. The second characterisation test is the VDA standard + high speed test. This test features a series of ten sinewaves with an amplitude of 50 mm. After extracting one cycle of each sinewave, the results can be displayed using a work diagram and characteristic diagrams. This gives insight into the force built up, the peak forces, the side-effects and hysteresis properties of the shock absorber. Both tests give a complete overview of all the characteristics of the shock absorber.

This report covers the enhanced shock absorber measurement procedure performed on the Ford LPG SAR. To process the results of this measurement procedure a post-processing tool has been developed which processes the data and visualises the data in a five page report.

Contents

1 Introduction

Ever since the automobile, or horseless carriage at that time, was introduced on the market there was some form of damping present in the suspension systems. At first this damping was introduced by dry friction either between layers of leaf springs or through the so-called snubbers. From 1925 onwards hydraulic dampers became dominant and to date hydraulics is still the main source to generate the damping force for most automotive applications [3].

Ride comfort in cars in an important design consideration. It can be classified in terms of vibrations that could be perceived as uncomfortable by its occupants. To quantify ride comfort, it is commonly accepted to look at the duration of time the human body can comfortably withstand a vibration of a certain frequency. This relation between the duration and frequency of a certain whole body vibration is set forth in the international standard ISO 2631-1 [10]. The vibrations perceived by the occupants of the car are either caused by the roughness of the road surface or generated on-board [5]. The on-board generated vibrations are for instance caused by rotating components in the car such as the engine or driveline. Another source of on-board vibrations are for instance the body motions or vibrations of the unsprung mass. The spring-damper combination in the suspension system of a modern car is designed to control the body motions and reduce the vibrations in the vehicle caused by the roughness of the road or the unsprung mass. To reduce shocks or vibrations, the spring absorbs the shock while the damper dissipates the energy of the shock. In contrast to its function, the term shock absorber is used in this report to refer to this damper component.

The main contribution of the internship was to enhance the shock absorber measurement procedure with the Ford Lommel Proving Ground (LPG) shock absorber rig. Secondly, an easy to use post-processing tool was developed resulting in a five page report visualising the results of the shock absorber measurements.

In chapter 2, an introduction into automotive shock absorbers and why shock absorbers are used in automotive is given. Next, an introduction into how shock absorbers are tuned to exhibit a certain damping force behaviour is given. In chapter 3, the setup of the shock absorber rig at Ford LPG is shortly introduced together with a report on how the machine is tuned to perform the standardised shock absorber measurement procedure. This measurement procedure is explained in chapter 4. After a measurement is performed, the results that are captured have to be processed (post-processing), this is covered in chapter 5.

2 Automotive Shock Absorber

An automotive shock absorber generates a damping force to damp out motions of the car. Section 2.1 explains the basic working principle of a passive shock absorber. After this, in section 2.2 the two main types of automotive shock absorbers are introduced. In section 2.3 the main purpose of automotive shock absorbers is set forth. Lastly, an insight into how shock absorbers are tuned to serve their purpose in the best possible way is given in section 2.4.

2.1 Principle

Shock absorbers dissipate the energy of a shock by transforming its energy, introduced by the velocity of the shock absorber rod, to another form of energy. This other form of energy is usually heat due to friction. A conventional automotive shock absorber introduces controlled friction to dissipate the energy. There are three types of friction that can be identified [3]:

1. fluid viscous friction
2. fluid dynamic friction
3. dry solid friction

Fluid viscous and fluid dynamic friction are the main types of friction in a conventional hydraulic shock absorber. Designers of such shock absorbers control these friction components by forcing hydraulic fluid through valves and orifices. Fluid viscous and fluid dynamic friction are proportional to the flow rate of a fluid, Q, as shown in (1). Fluid viscous friction, F_{visc}, depends on fluid viscosity while fluid dynamic friction, F_{dyn}, rests on the principle of energy dissipation from turbulence.

$$F_{visc} \propto Q \quad and \quad F_{dyn} \propto Q^2 \tag{1}$$

Dry solid friction, also known as Coulomb friction or static friction F_{static}, is friction between two solid materials. The magnitude of the friction force depends on the coefficient of friction, μ_F, between the two materials. One would like to minimize this type of friction as much as possible because it is an uncontrolled form of friction which tends to lock movement at low speeds. This locking can cause unwanted vibrations or stick slip behaviour.

As indicated by (2), these three types of friction contribute to a total damping force, $F_{damping}$. To characterise a shock absorber one would like to gain insight into the magnitude of this damping force at certain speeds and displacements. Chapters 4 and 5 give insight into how this damping force is measured and visualised.

$$F_{damping} = F_{static} + F_{visc} + F_{dyn} \tag{2}$$

2.2 Types

For more than half a century, telescopic shock absorbers have been used in automotive applications. As illustrated in figure 1, three types of telescopic shock absorbers can be distinguished: through-rod, double-tube (or twintube) and single-tube (or monotube). Nowadays, most trade-offs are made between the twintube and monotube type. The through-rod type is usually neglected because it requires the need for external seals at two ends (which are subject to high pressures), the protruding end may be inconvenient or dangerous and there is no provision for the thermal expansion of the oil [3]. For this reason, the through-rod type will not be discussed any further. The monotube and twintube type are discussed in more detail below.

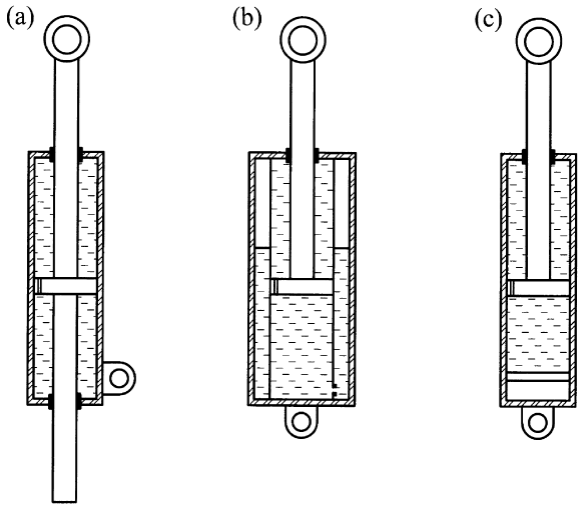

Figure 1: Three types of a telescopic damper: (a) through-rod; (b) double-tube and (c) single-tube [3]

2.2.1 Monotube

The monotube damper is known as the typical passive shock absorber. It features a working chamber containing the hydraulic fluid, usually oil, and a closed gas chamber containing pressurised gas (air or nitrogen are commonly used) separated by an independent floating piston. A schematic of a monotube damper is given in figure 2.

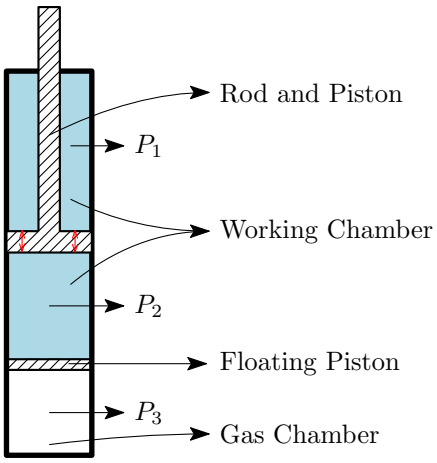

Figure 2: Schematic of a monotube damper

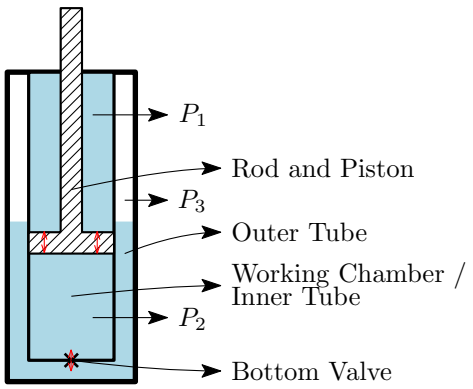

Figure 3: Schematic of a twintube damper

In the most basic way it can be said that the damping force generated by the shock absorber is built up from the forces acting on the bottom and the top of the piston. The force acting on the bottom of the piston is expressed as

$$F_{bottom} = P_2 \cdot A_{tube} \tag{3}$$

and the force acting on the top of the piston is given by

$$F_{top} = P_1 \cdot (A_{tube} - A_{rod})\,. \tag{4}$$

In (3) and (4), A_{tube} refers to the cross-sectional area of the tube and A_{rod} refers to the cross-sectional area of the rod.

The damping force in jounce motion, in other words compression of the shock absorber, is given by

$$F_{jounce_{mono}} = F_{bottom} - F_{top}. \tag{5}$$

The damping force in rebound motion or extension of the shock absorber, is given by

$$F_{rebound_{mono}} = F_{top} - F_{bottom}. \tag{6}$$

As can be seen from (3) to (6), the pressure above and below the piston result in a damping force. There are two contributions to these pressures: firstly the gas pressure and secondly the pressure difference across the piston. The gas pressure is dependent on the stroke and temperature. The pressure difference across the piston is created through hydraulic restriction and it is proportional to the flow rate of the liquid through the piston [12]. The restriction in a damper is obtained by creating a stack of discs acting as a valve which will be elaborated upon in section 2.4.

The main functions of the gas in a monotube damper are firstly to allow rod-insertion and secondly to prevent cavitation [12]:

1. When the shock absorber is compressed (jounce motion), a section of the rod enters the working chamber. The volume of this section is accommodated by compressing the gas because the compressibility of the liquid is limited. Assuming the gas is compressed isentropically, the dependency of gas pressure on stroke is given by

$$P_{gas} = P_{gas,0} \left(\frac{V_{gas,0}}{V_{gas,0} - xA_{rod}} \right)^n \tag{7}$$

   with $P_{gas,0}$ the initial gas pressure at mid-stroke, $V_{gas,0}$ the initial gas volume at mid-stroke, x the length of rod inserted with respect to mid-stroke and n the polytropic index which is equal to 1.4 for air under isentropic conditions.

2. When the required movement of the working fluid becomes too high (stroke velocity too high), vacuum bubbles are formed what is known as cavitation. To prevent cavitation, the gas pressure should be higher than the pressure difference across the piston. Cavitation is an unwanted side effect because it causes a force lag and unwanted noise (for instance knocking) inside the vehicle. The lag in force build up occurs because the vacuum bubbles first have to be compressed before the liquid can flow through the piston.

2.2.2 Twintube

The twintube damper is built up with an inner and an outer tube. The outer tube contains the gas and is separated from the working chamber by a valve. Where for a monotube damper the gas is separated completely from the liquid, there is direct contact between the liquid and gas in a twintube damper. This means that the liquid and gas will be mixing to some degree. A schematic visualising a twintube damper is given in figure 3.

There are two types of twintube dampers commonly sold for automotive applications: twintube rod displaced and twintube full displaced [12].

1. The rod displaced damper in jounce motion has unrestricted flow around the piston but restricted flow through the base valve. The damping force is then created by the pressure acting on the rod area given by

$$F_{jounce_{rod}} = P_2 \cdot A_{rod} \tag{8}$$

   while

$$P_2 \propto Q_{base}^2 \tag{9}$$

with Q_{base} representing the flow rate through the base valve. Moreover, the pressure is equal throughout the working chamber. In rebound motion, the flow is restricted at the bottom of the piston and the working chamber is replenished with free flow through the base valve aided by the gas pressure. The damping force in rebound is created in the same way as with a monotube damper and is equal to

$$F_{rebound_{twin}} = F_{top} - F_{bottom}. \tag{10}$$

2. The full displaced damper works in the same way as the rod displaced damper, however, there is an additional flow restriction through the piston. The damping force is then equal

$$F_{jounce_{twin}} = F_{bottom} - F_{top}. \tag{11}$$

with the main difference that P_2 is both proportional to the flow rate squared through the piston and the base valve. This requires the need to check the hydraulic balance of the damper. If the restriction around the base valve and around piston are too tight, the volume above the piston cannot be replenished fast enough at high stroke velocities and large strokes. This causes cavitation to occur.

2.3 Shock Absorber Purpose

With the development of automotive shock absorbers there is always a fundamental trade-off between performance (safety) and comfort. The performance plays a key role in keeping a good tyre-to-road contact which is essential for handling and vehicle control necessary for safe travel. This performance setting is a "harder" setting, pressing the four tyres to the ground, which is unfavourable for comfort [12, 1, 4]. Comfort can be quantified as the exposure of the human body to whole-body vibration. This is quantified by the International Standard ISO 2631-1 and it states that the human body is most sensitive to vertical vibrations in the range of 4-8 Hz [10].

Let us look further into why dampers are used in automotive. A damper should [8, 9]:

1. damp out low frequency body motions ($\sim$ 0.5 to 4 Hz, figure 4(a))
2. not transmit "high" frequency road input also known as choppiness ($\sim$ 4 to 7 Hz, figure 4(b))
3. damp out vibrations of unsprung mass such as suspension shake ($\sim$ 8 to 20 Hz, figure 4(c))
4. not exceed "normal" levels of abruptness, which is determined subjectively by expert drivers
5. not generate vibrations or noise

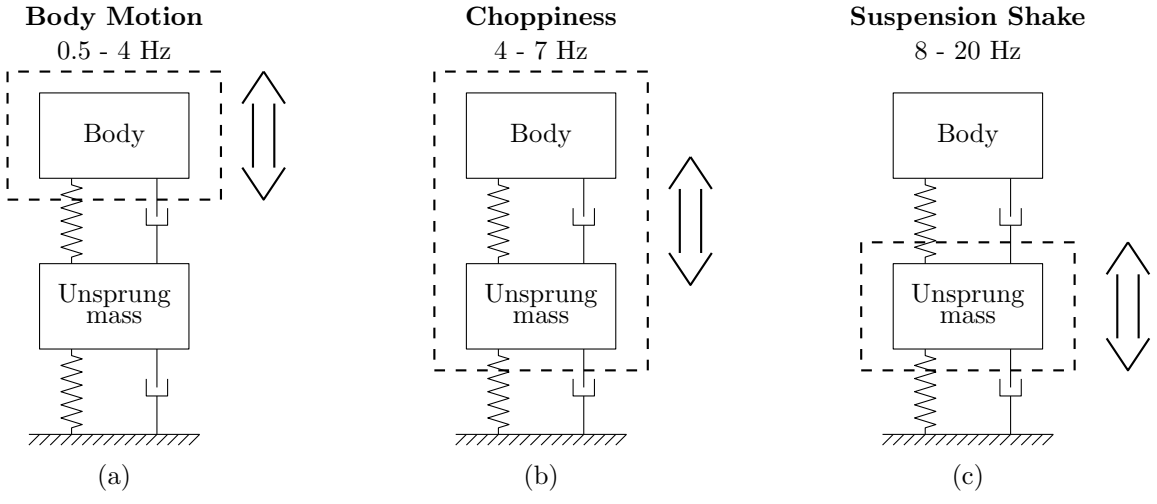

Figure 4: Graphical representation of (a) body motion, (b) choppiness and (c) wheel modes

To handle the eigenmotions depicted in figure 4 in the best way, one would like to have high damping to counter the body motion and shake but low damping to counter choppiness. The reason one wants to have low damping for choppiness is because it is a vibration transmitted due to the fixation of the suspension. This fixation increases if dampers are tuned for a "harder", i.e. high damping, setting. Note that the choppiness metric lies in the vibration range where the human is most sensitive to vibrations [10]. Because of this, a difficult trade-off arises: either have a high damping to control the body motions and shake (good for performance and safety), but increase choppiness (reduce comfort), or have low damping, to reduce choppiness (increase comfort) but have uncontrolled body motions and shake (bad for performance and safety). This trade-off is visualised in figure 5.

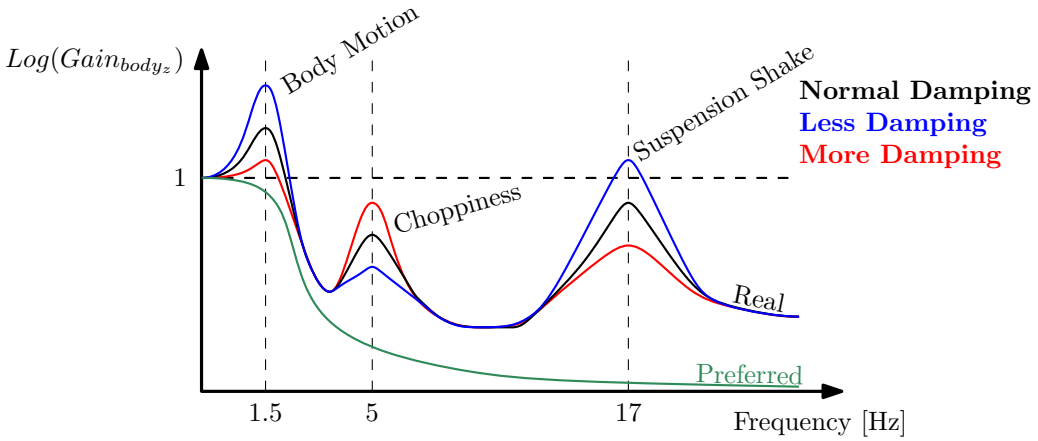

Figure 5: Trade-off for damping the main eigenmotions [8]

2.4 Shock Absorber Tuning

Automotive shock absorber tuning is mainly performed by changing the valve characteristics around the piston. The piston valves are created by stacking discs on top of each other. Each disc has a certain stiffness and a certain lay-out of holes or cut-outs. An illustration of a disc stack is shown in figure 6. Furthermore, the disc stacks are composed of different discs for rebound and jounce motion to be able to tune the damping of these motions separately. A schematic of a general piston lay-out is shown in figure 7.

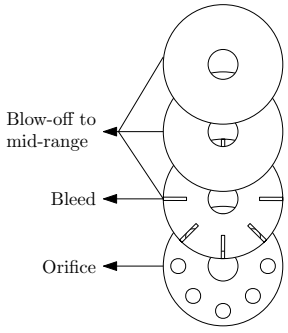

Figure 6: Graphical representation of a disc stack with orifice

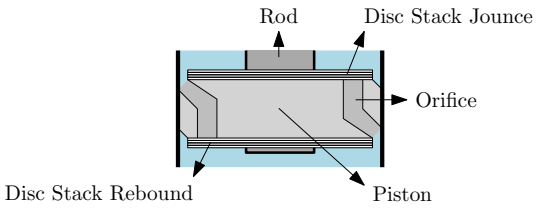

Figure 7: Schematic of the piston with the two disc stacks

To get a feel for how a certain disc stack lay-out influences the damping force, one can look at figure 8. The figure shows how the size of the holes, a stiffer disc stack and the preload put on the disc stack influences the damping force. The figure also introduces four regions in the force-velocity graph: bleed, blow-off, mid-range and orifice.

- A bleed disc always allows flow to pass through the piston valve. At low speeds, the pressure difference across the piston is not large enough to allow the disc stack to bend upwards and allow oil flow through the piston valve. The bleed disc makes sure that there will always be a small amount of flow. Because it only affects low speed behaviour, it influences the early transient body modes such as bounce, pitch and roll. To influence the control of these body modes, one can replace the bleed disc with one that has either an increased of decreased slot area.
- Blow-off indicates the behaviour of the shock absorber at the moment the disc stack opens to allow oil flow through the piston valve. The blow-off characteristic can be influenced by the amount of preload put on the disc stack. Preload signifies how much moment is put on the top disc, squeezing the disc stack onto the piston and requiring a larger pressure difference to open the piston valve. Blow-off influences the primary body modes, suspension shake and choppiness.
- Mid-range signifies the performance of the shock absorber at medium to high speed. The stiffness of the disc stack influences the behaviour at these speeds. Like blow-off, mid-range influences the primary body modes, suspension shake and choppiness.
- The high speed behaviour of the shock absorber is influenced by the orifice. The orifices are the canals through which the oil flows to the disc stack. The orifice area influences choppiness behaviour and the maximum damping force the shock absorber can create.

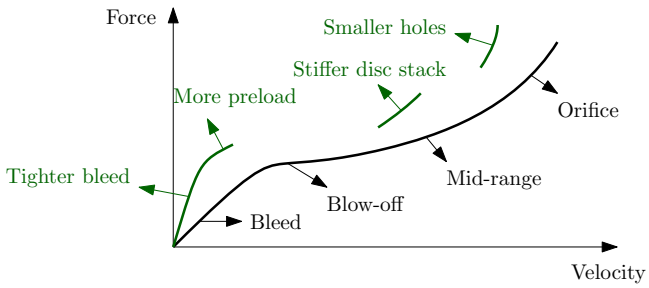

Figure 8: Disc stack influence on damping force [12]

Tuning of shock absorbers at LPG is performed by expert drivers. They assess different valve designs and determine the final configuration. They perform the assessment in a subjective way by driving the car on the LPG test tracks. Final tuning is performed on challenging public roads to guarantee optimal comfort and performance. Each car model will have differently tuned shock absorbers and in many cases also different versions of a certain model get a custom tune. Subjective tuning of shock absorbers is required because the findings of subjective vehicle tests and objective component measurements are difficult to correlate. In other words, a component measurement does not give insight into the unwanted vehicle motions which requires subjective vehicle tests to define the tune of the shock absorber.

Lastly, it is important to note that gas pressure and, in case of twintube shock absorbers, base valve design also have an influence on the damping force generation over the entire speed range. However, tuning the gas pressure and base valve is mainly performed to overcome unwanted effects such as cavitation and knocking.

3 LPG Shock Absorber Rig

Automotive shock absorber tuning nowadays is mainly performed by changing valve discs in specialised development dampers as was explained section 2.4. Next, these dampers are mounted into a car to be evaluated subjectively. To gain valuable and objective insight into the performance of a certain valve configuration, a shock absorber rig can be used. Section 3.1 gives information on the shock absorber rig at LPG. How this rig can be tuned for performance is shown in section 3.2.

3.1 Servo-Hydraulic Shock Absorber Rig

The test rig at LPG is a servo-hydraulic shock absorber rig (SAR). It has recently been updated with new hardware and software. The setup is provided by MTS Systems and consists of a frame to mount the damper, a hydraulic actuator, a three-stage servovalve unit, a hydraulic power unit (HPU), three accumulators, a controller and a PC. At the top of the frame a calibrated load cell is placed to measure the force the damper exerts. An overview of the setup at LPG is shown in figure 9.

Next to the force and axial displacement readout, the controller allows up to 14 extra sensor signal inputs. In this case a thermocouple is added. It is also possible to use the controller to control three extra channels. This could be interesting to be able to test continuously controlled dampers which can vary their damping characteristics.

A schematic of the hydraulic system of the SAR is given in figure 10. It can be seen that the HPU supplies the three-stage servovalve unit with hydraulic fluid through three hydraulic accumulators. The hydraulic accumulators are store hydraulic fluid and contained nitrogen gas which is separated by a floating piston. The nitrogen is precharged at 16 bar and its function is to filter out fluctuations in the hydraulic lines and provide a steady hydraulic pressure. Being able to filter out these fluctuations is necessary because the three-stage servovalve unit enables very high flow rates to the hydraulic actuator. If high oil flow rates are not desired it is possible to manually restrict the oil flow of two of the three servovalves. The controller controls the hydraulic actuator using the servovalve unit and the actuator position measurement.

To program the hydraulic actuator, one can either use standard inputs with their MPT (Multipurpose Testware) software or your own timed displacement input. For the scope of this internship, it was chosen to implement the measurement procedure using MPT. Chapter 4 covers the measurement procedure that has been implemented with MPT. The SAR can also be used for testing other products. One example is the dynamic characterisation of spring aids which is discussed in appendix B.

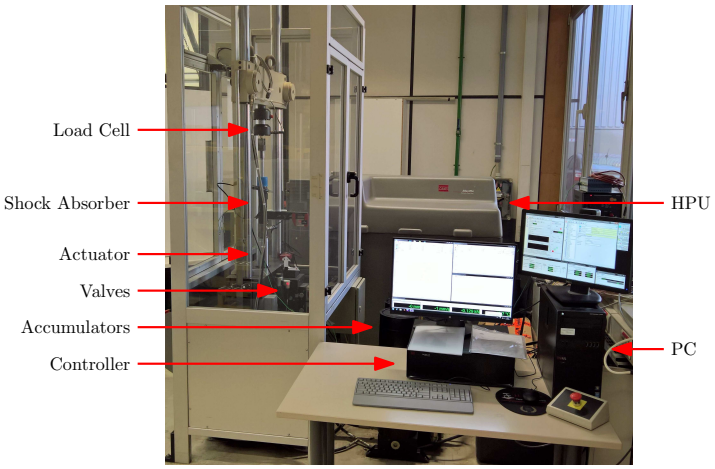

Figure 9: LPG shock absorber rig

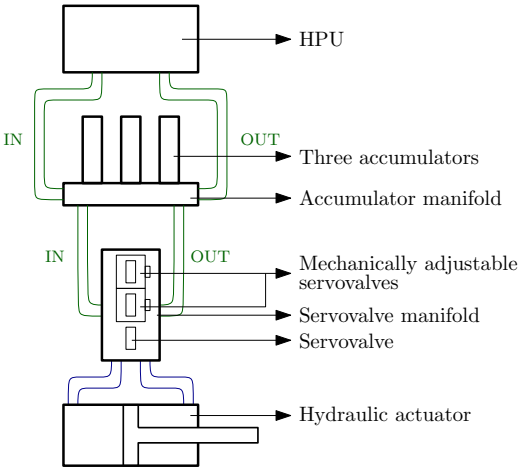

Figure 10: SAR Hydraulic system

The outputs of the rig are recorded at a sampling frequency of 1024 Hz. The outputs for the damper characterisation measurements are listed below, note that the outputs are recorded according to the Ford engineering specification [6]:

1. Time [s]
2. Measured axial displacement [mm]
3. Axial displacement Input [mm]
4. Axial velocity [mm/s]
5. Force [kN]
6. Temperature [°C]

3.2 Rig Tuning

The performance of the rig is very much dependant on how it has been tuned. It is influenced by two main factors: the PID tune of the controller and the mechanical opening of the two manually adjustable servovalves. Because of the nature of the tests that will be discussed in chapter 4, it was chosen to completely open the servovalves. The test procedure features large amplitudes at high stroke velocities requiring a maximum hydraulic oil flow.

In order for the tuning of the rig to be performed in a time efficient manner, the built-in advanced PID tuning function of the MTS Software is used. Before the tuning session can be started it is important to understand which tests are going to be performed. The damper characterisation tests will be discussed in chapter 4. It is important to note that the main test contains a series of sines with an amplitude of 50 mm.

There are three main parameter inputs to the advanced tuning: the amplitude limit, tracking percentage and sweep frequency [2]. The tuning procedure is the following:

1. First, the actuator slowly ramps up and down to 80% of the amplitude limit to determine basic PI gains
2. After basic PI gains are determined, a frequency sweep is performed to determine the final PID gains. This frequency sweep has a maximum frequency defined by the sweep frequency input, the amplitude equals 20% of the amplitude limit.

The tracking percentage is a metric, introduced by the MTS Software, to signify how aggressive the actuator tracks the command input. Default value is 50%, increasing the tracking percentage may lead to unstable PID gains [2].

To gain an insight into how well a certain tune performs, two testsignals were used: a 2.5 mm amplitude block signal oscillating at 1 Hz and a sinewave containing five cycles of a medium (524 mm/s) and five cycles of a high (1571 mm/s) stroke velocity sinewave. These two velocities are chosen from the characterisation test procedure that will be set forth in chapter 4. From these two sinewaves, the second to last cycle is extracted to allow ramp down in the last cycle. The second to last cycle is then used to check the deviation of the amplitude and peak velocity. These are checked because thy are important metrics in the final test procedure. Figure 11 graphically shows the three amplitudes and two strokes that are extracted. The peak velocity is found at mid-stroke of the two strokes and is checked for both rebound and jounce.

Table 1 shows five tunes that have been evaluated. All tunes consider an amplitude of 50 mm because this is the amplitude used in the main tests. Tune 1 corresponds to the recommended parameters to start tuning according to the MTS system software manual [2]. Because of the large amplitudes that were imposed during the 20 Hz sinesweep a large resonance was found at around 18 Hz. This caused the machine to shake violently which resulted in the decision to lower the frequency sweep to 15 Hz for tune 2. Tune 3 to 5 checked the influence of increasing and decreasing the tracking percentage.

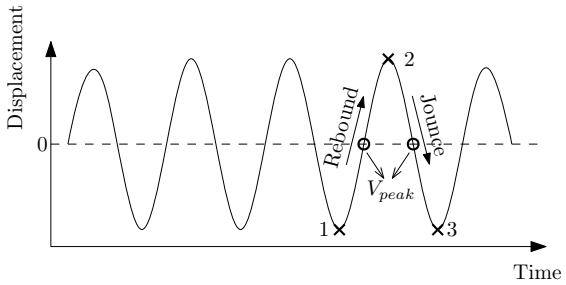

Figure 11: Extraction of fourth cycle with three amplitudes of interest and two peak velocities at mid-stroke

Table 1: Tuning inputs and resulting PID gains

	Amplitude [mm]	**Tracking** [%]	**Sweep** [Hz]	**P**	**I**	**D**
Tune 1	50	50	20	3.050	0.610	0.00305
Tune 2	50	50	15	3.115	0.623	0.00304
Tune 3	50	55	15	3.286	0.657	0.00306
Tune 4	50	30	15	2.247	0.449	0.00458
Tune 5	50	10	15	1.585	0.317	0.00597

Before continuing the discussion of table 2, it is important to set the minimum requirements that the tuned rig must meet. Firstly, the stroke length must be at least 100 mm. In other words, the amplitude has to be at least 50 mm. Secondly, the peak velocity should not deviate more than 1%. Note that the tuning is performed without a damper attached which results in these tight requirements.

Table 2 shows the deviations in peak velocity and amplitude. As can be seen in the table, the peak jounce and rebound velocities of tune 1 are within the limits. However, at high speed, the stroke marginally does not attain 100 mm. With tune 3 the objective was to try to increase the tracking percentage as high as possible. A stable solution was found up to 55% tracking. The increased proportional gain however causes the rebound velocity at high speed to be out of bounds. The effect of this higher proportional gain can be seen in the overshoot peak of the darkblue line in figure 12. Tune 4 and 5 represent lower tracking percentages in figure 12. Although they do not show any overshoot behaviour or oscillations, they are unable to attain the stroke velocities and amplitudes, especially at high speeds. As a result, tune 2 is chosen as the best performing configuration and the corresponding PID gains will be used for the standard characterisation test.

Table 2: Peak velocity and amplitude deviations (negative values signify the value is too low)

	Velocity [mm/s]	**Jounce** [%]	**Rebound** [%]	**Amplitude 1** [%]	**Amplitude 2** [%]	**Amplitude 3** [%]
Tune 1	524	0.11	0.26	0.22	0.20	0.19
	1571	0.48	0.58	-0.10	0.01	-0.14
Tune 2	524	0.14	0.25	0.24	0.22	0.23
	1571	0.47	0.80	0.04	0.07	-0.02
Tune 3	524	0.11	0.28	0.22	0.26	0.22
	1571	0.65	1.09	0.32	0.36	0.18
Tune 4	524	-0.17	-0.06	-0.04	-0.04	-0.09
	1571	-2.70	-2.24	-3.25	-2.88	-3.31
Tune 5	524	-1.21	-0.83	-1.02	-0.79	-1.05
	1571	-9.98	-9.64	-10.64	-9.78	-10.78

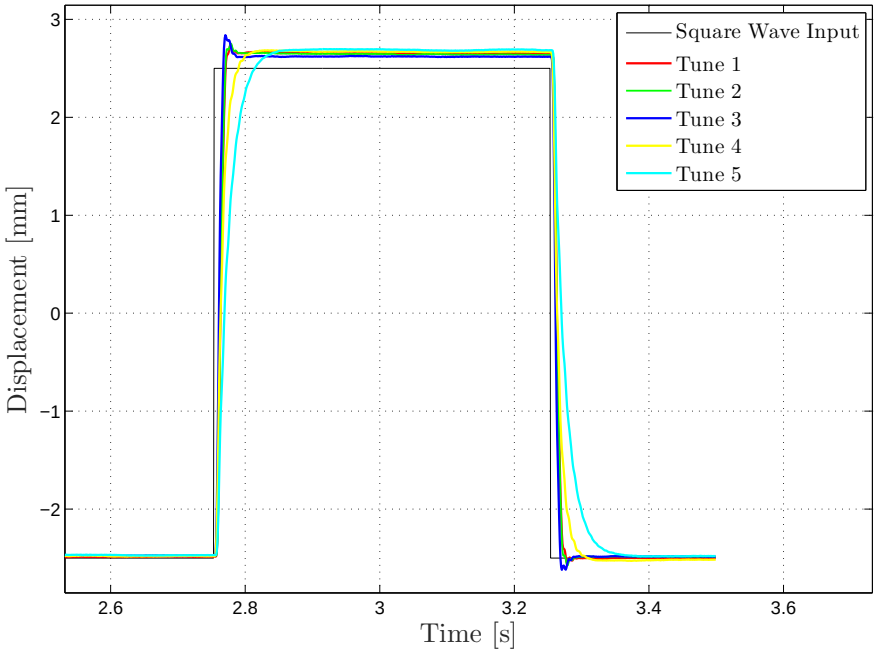

Figure 12: Difference in tune configuration for a rebound square wave

4 Measurement Procedure

The basic set of checks and measurements that are implemented for the characterisation procedure of a shock absorber are covered in this chapter. As a starting point in setting up the measurement procedure, the Ford Motor Company Core Engineering Specification (CES) is used as a base [6]. In this document the overall circumstances in which the test should be performed are listed. Examples of these overall circumstances are: check if the shock absorber is clean and undamaged, check the ambient temperature, etc. The CES mainly covers how the friction and gas test should be performed, and which stroke velocities and amplitudes should be used to determine the force characteristics of the shock absorber. The four main parts of the test procedure set-up during this internship are the lock check, the temperature check, the friction and gas test, and the VDA standard + high speed test. These four tests are discussed in sections 4.1 to 4.4 respectively.

4.1 Lock Check

The lock check is added to ensure safe operation of the rig and to prevent damage to the shock absorber. At a stroke velocity of 2 mm/s the cylinder of the hydraulic rig moves to the limit bounds. These bounds are +50 mm (maximum extension) and -50 mm (maximum compression). During the movement the rig monitors the force built up. When the force becomes too high (> 300 N), for instance when the shock absorber reaches its end stops due to wrong alignment in the machine, the programme stops. This makes sure both the rig and the shock absorber do not get damaged.

4.2 Temperature Check

The next check comes from the requirement stated in CES that shock absorber should be 23°C (±3°C). In most cases, and this is always preferred, the shock absorber is soaked in this temperature for at least 24 hours. Because this is not always possible the temperature check is added. When the temperature, measured with a thermocouple at the shock absorber housing as explained in the next paragraph, is below 22°C, a warm-up sequence is started. The rig starts a sine oscillation of 2 Hz with an amplitude of 50 mm until the shock absorber reaches a temperature of 22°C. This takes into account a delay in the temperature built-up which results in the specimen to be $\approx$ 23°C at the start of the tests.

From figure 2, it became clear that monotube dampers have a gas chamber at the bottom. Due to the fluid viscous and fluid dynamic friction, the temperature of the oil is most important and therefore the thermocouple should be placed at the location where the oil flows. The thermocouple is therefore taped to the housing of the shock absorber at the location of the working chamber. A good rule of thumb to make sure the location is correct is to place it at approximately 1/3 of the length of the housing measured from the bottom. This location is also used for twintube dampers (figure 3), although in this case the thermocouple could also be placed lower.

To get a feel for the effect of temperature on the test results a temperature sweep has been performed. A shock absorber was cooled down and then the standard tests, which will be described in section 4.3 and 4.4, were performed. Each time the test is performed the starting temperature is increased by 3 °C. The sweep of starting temperatures that have been achieved ranged from 13 to 40 °C. The shock absorber that was tested in this case was a twintube shock absorber.

Figure 13 shows the temperature dependency of the friction and gas test. The most significant result can be found in the gas force deviation (top left). This shows that the gas force linearly increases with temperature. This is conform to the ideal gas law. In terms of friction, deviations up to 8.5% can be observed. The friction is the lowest in all cases around 30 °C for this shock absorber. However, other shock absorbers can have different types of seals and can have other optimum temperatures for friction. From this test it can be concluded that friction in shock absorbers can have a temperature dependency, however the influence on force generation can be neglected due to the fact that maximum forces at high speed can reach several kilonewtons while the influence on friction is only a couple newtons. The influence of temperature on gas force, however, is significant which signifies the importance of using a temperature requirement.

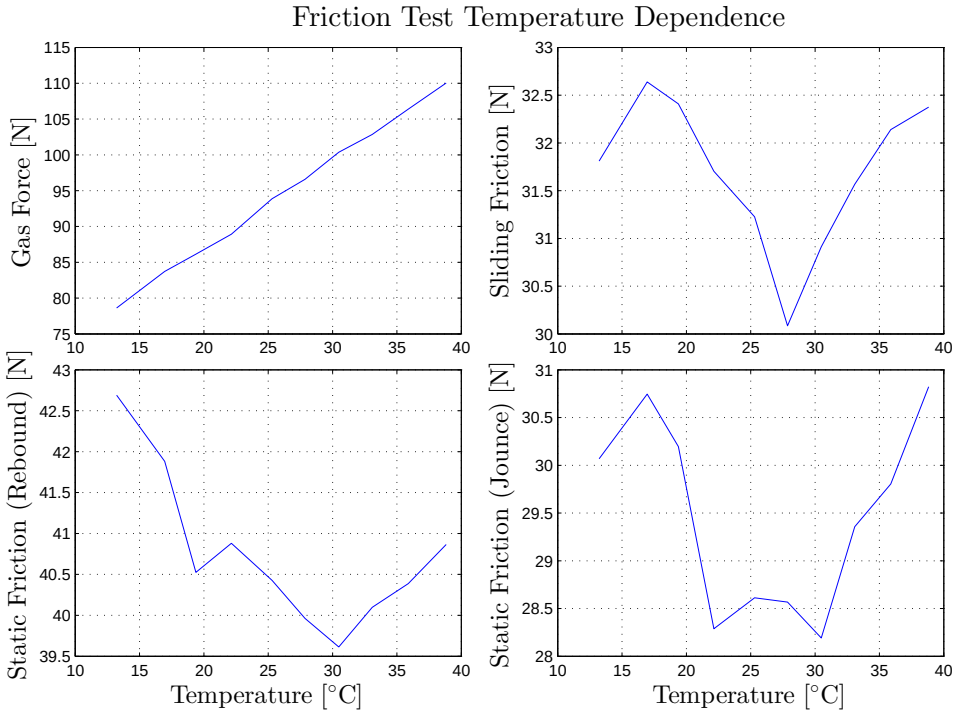

Figure 13: Temperature dependence of friction and gas test

It is important to note that the temperature does not remain constant during testing. This can be seen in figure 14. Because of this only the starting temperature is monitored. The starting temperature is the temperature before the start of the friction and gas test. Immediately after the friction and gas test the VDA standard test is performed. Both tests are discussed in sections 4.3 and 4.4. There are two factors contributing to the temperature variation, firstly the nature of the test, and secondly the ambient temperature.

1. The friction and gas test is performed at a very low stroke velocity which means that the ambient temperature is dominant. However, due to the dynamic nature of the VDA standard test, the oil flow plays a significant role. This influence becomes clear from the top left and bottom left graph in figure 14. It can be seen that especially at the high starting temperatures there is a large variation in temperature with the friction and gas test while this variation is much lower with the VDA standard test.

2. The ambient temperature when the tests were performed was $\approx$ 21 °C. Looking at the top left graph in figure 14, a temperature drop of 2 °C can be observed at a starting temperature of 40 °C. This happens because of the large difference between the starting temperature and the ambient temperature.

The graphs on the right side of figure 14 show the deviation of the maximum and minimum temperature recorded during the test from the starting temperature. Note that at high starting temperatures, the maximum temperature during the VDA standard test is already lower than the starting temperature. This can be explained by the fact that the friction and gas test is executed before the VDA standard test. During the friction and gas test the shock absorber cools down due to the low ambient temperature.

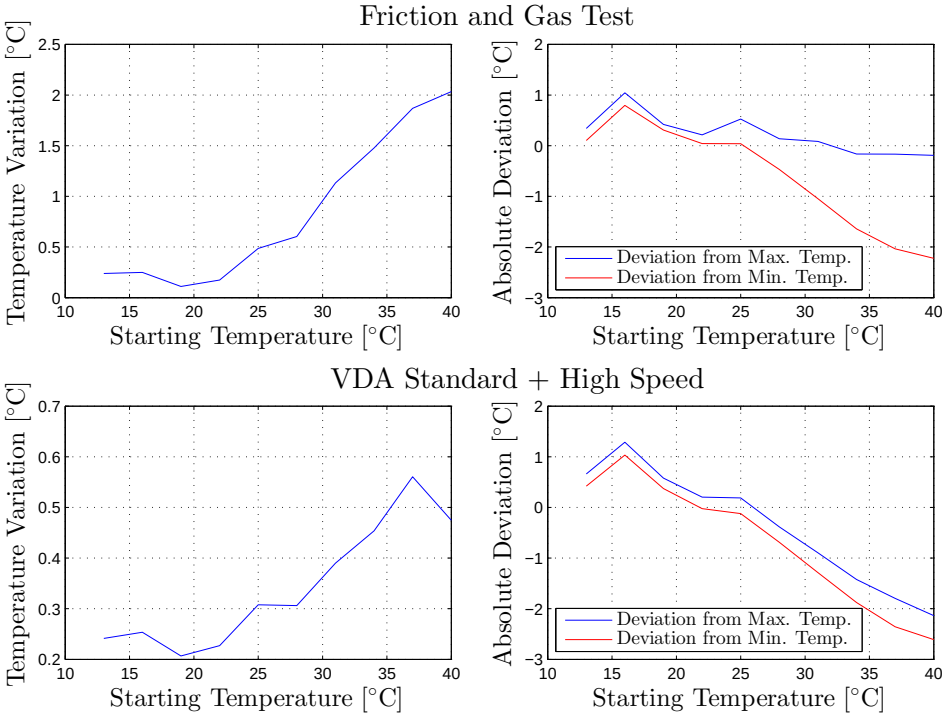

Figure 14: Temperature variation during the measurements

Lastly, the effect of temperature on the damping force generation is investigated. Figure 15 shows the force at peak velocity variation with temperature for the VDA standard test speeds. Note that among the different tests the peak velocities did not deviate more than 0.4% at 1590 mm/s, at lower speeds this deviation was even less. Next, a distinction is made between "normal" and "gas corrected". Gas corrected signifies that the gas force, derived in the friction and gas test, is deducted from the force. Since this gas force is a jounce force (this will become clear in section 5.1), the jounce force will effectively be lower, while the rebound force will effectively be higher.

In "normal" conditions, there is a tendency towards a decreasing rebound force and increasing jounce force. At high speeds this effect becomes less profound. This can be explained by the fact that the gas force increases with temperature. The fact that the gas force is a jounce force results in increasing the the forces in jounce and decreasing the forces in rebound. The fact that this effect becomes less profound at high speeds is because the flow of oil is a much more dominant contribution to the damping force.

When the total force is corrected with the gas force offset, one looks effectively only at damping force generated by the flow of oil through the valves. In this case there is an overall tendency for the damping force to reduce both in rebound and in jounce. This tendency can be rationalised by the viscosity of the oil flowing through the valves. As the temperature increases, the viscosity of the oil decreases. This decreases the fluid viscous friction causing the oil to more easily flow through the valves and thereby reducing the pressure difference which results in the damping force being lower.

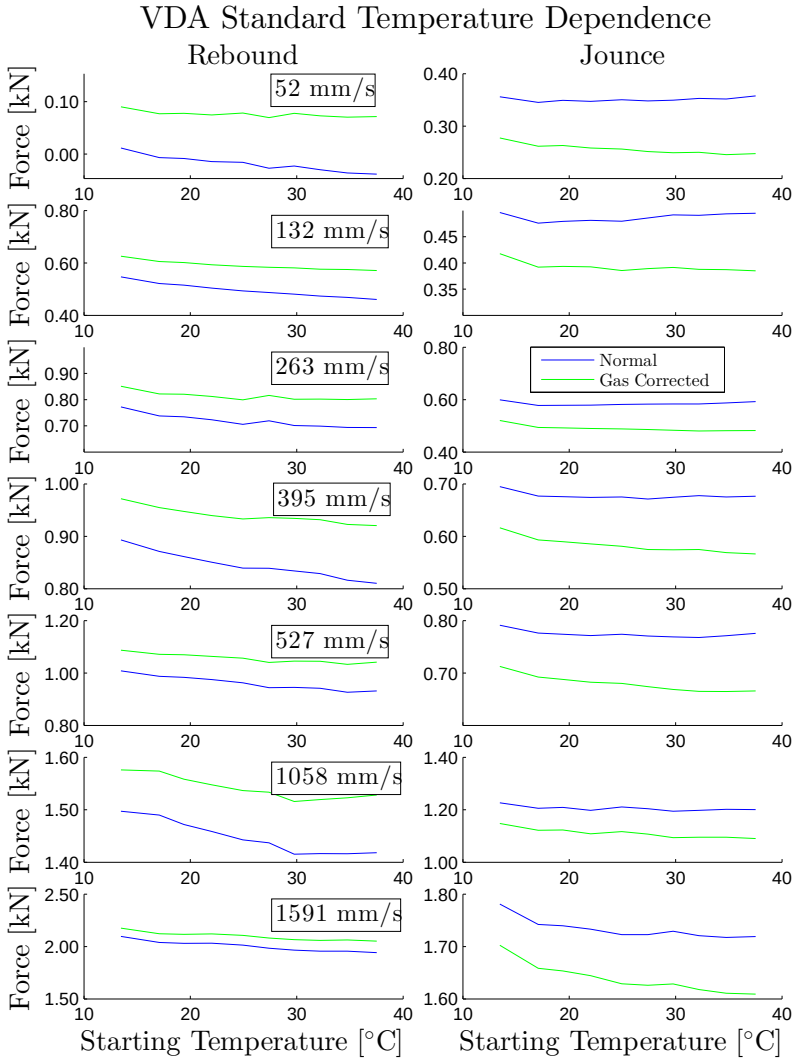

Figure 15: Temperature dependence of the force at peak velocity with gas force correction (green) and without gas force correction (blue)

To conclude this temperature section, it can be said that temperature plays an important role on the results of the tests. Therefore, the warm-up sequence to get the specimen up to a temperature of ≈ 23 °C is definitely a positive addition to the measurement procedure to increase robustness. Next to this, the ambient temperature of the room should be kept constant at ≈ 23 °C as well. Because it is not always possible to have both temperatures within range, it is chosen to document the specimen temperature at the start and end of the test in the post-processing graphs which are discussed in chapter 5.

4.3 Friction and Gas Test

The friction and gas test is used to determine the friction forces and gas force of the shock absorber. High friction forces have a negative influence on the choppiness behaviour of the car. Before starting the test, the shock absorber is excited with five cycles of a sine wave with maximum stroke velocity of 100 mm/s and amplitude of 25 mm to prime the oil flow through the valves and cylinder according to the CES [6]. Note that an amplitude of 25 mm signifies the amplitude around the mid-stroke position of the shock absorber.

The actual test is a ramp up and down with an amplitude of 10 mm as shown in figure 16. To allow the hydraulics of the shock absorber to settle, a delay of 2 sec is added between the strokes. The measurement is started at the second stroke (jounce) and ends after the third stroke (rebound) [6]. The test is performed at a very low stroke velocity of 0.4 mm/s and this velocity has to be constant for at least 95% of the stroke. The low stroke velocity is used to minimize the effect of the fluid viscous and fluid dynamic friction. In other words, the effect of the oil flowing through the valves needs to be minimised to be able to measure only the influence of seal friction and gas force. How these friction forces and gas force are determined from the measurement data is explained in chapter 5.

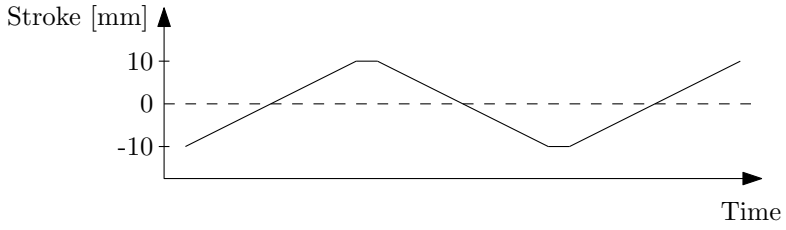

Figure 16: Friction and gas test sequence

4.4 VDA Standard + High Speed

The VDA standard + high speed test consists of a series of sines with an amplitude of 50 mm [6]. It is effectively a combination of the shock absorber characterisation speeds standardised by the German Association of the Automotive Industry (VDA) and three extra sines with a very high stroke velocity regularly requested by Ford Motor Company engineers. An overview of these stroke velocities and corresponding frequencies are given in table 3.

Table 3: VDA standard + high speed piston speeds and frequencies at a 50 mm amplitude

Peak Piston Speed [mm/s]	52	131	262	393	524	1047	1571	2000	2500	3000
Frequency [Hz]	0.1655	0.4170	0.8340	1.2510	1.6679	3.3327	5.0006	6.3662	7.9577	9.5493

Figure 17 shows the displacement input sent to the hydraulic actuator of the rig. As can be seen there are four cycles for each stroke velocity (piston speed). Between each set of oscillations, a delay of 1 sec is added. This delay allows for the accumulators to recharge with hydraulic oil. At the two highest stroke velocities, between 2000 and 2500 mm/s and between 2500 and 3000 mm/s, a delay of 1.5 sec is used because it was found that the accumulators needed more time to recharge for these very large velocities. Note that because the performance of the rig does not change and because otherwise the damper temperature increases more, the amount of cycles is decreased from five to four compared to section 3.2.

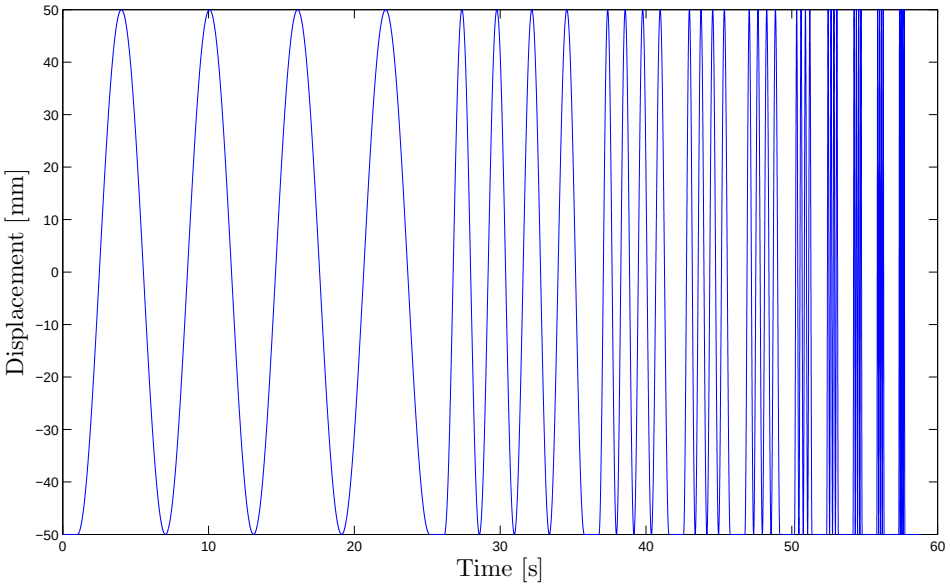

Figure 17: VDA standard + high speed axial displacement input

The purpose of the test is to get an understanding of the damping force generated by the shock absorber at each stroke velocity. Before starting the test, the shock absorber is set at mid-stroke and a force offset is taken. This is done to compensate for the gas force. During the test, the force is continuously measured using the load cell attached to the frame. However, every second to last cycle is extracted to process the results. This is done to allow the machine to have a short ramp up/down at the start/end of the oscillation. The second cycle is used to make sure the dynamic behaviour of the shock absorber is tested. The results can then be visualised in several ways as will be explained in chapter 5.

5 Post-processing

After the measurements are performed, the results have to be reported in a standardised way. This chapter covers the different methods that are used to visualise the data and the calculations that are related to the processing of the data. Section 5.1 covers the friction and gas forces measured during the friction and gas test. Next, the work diagram is discussed in section 5.2, followed by the characteristic diagram in section 5.3. As a last page in the reports, the performance of the rig during the test is evaluated in section 5.4. The final shock absorber test report, an example of which is shown in appendix A, consists of five pages: one friction and gas test page, one page containing the work diagram, two pages with the characteristic diagrams and speeds table, and lastly, one page covering the performance of the rig.

5.1 Friction and Gas Forces

Using the data gathered during the friction and gas test procedure set forth in section 4.3, the friction and gas forces can be determined. There are three friction forces that are of interest: the sliding friction, the static friction when extended and the static friction when compressed [6]. The output figure consists of a force versus displacement graph. The raw data figure is presented in figure 18. To get usable output data the force signal needs to be filtered using a low-pass filter. The chosen filter is a Butterworth filter because it has a very flat frequency response in the passband. The cut-off frequency that yielded satisfactory results was 2 Hz after which the response decreases linearly to negative infinity. The slope with which it decreases linearly is equal to -54 dB per octave corresponding to a ninth order.

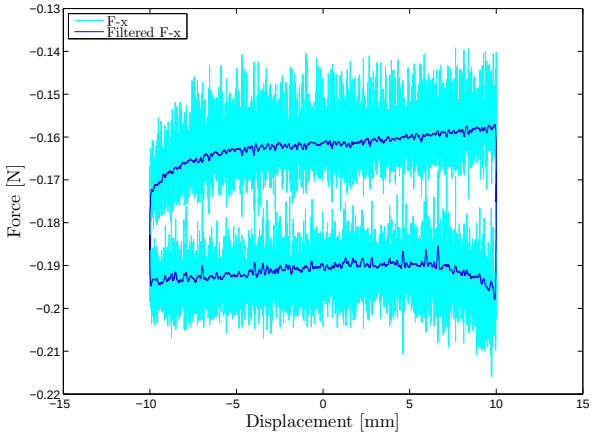

Figure 18: Friction and Gas Test filtered force signal using a ninth order low-pass Butterworth filter with a cut-off frequency at 2 Hz

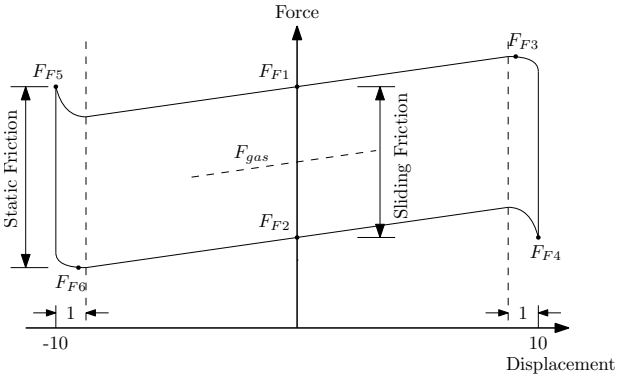

Figure 19: Friction and Gas force determination [3, 6]

After filtering the force signal, the friction forces can be determined. Figure 19 illustrates how to determine the sliding friction and static friction (stiction) using the six friction force components F_{F1} to F_{F6}. Note that the filtered signal from figure 18 is not exactly follow the shape of figure 19. The reason for this will become clear later in this section. The sliding friction is measured around the mid-stroke of the shock absorber and can be calculated by subtracting F_{F2} from F_{F1} (12).

$$F_{slide} = F_{F1} - F_{F2} \tag{12}$$

The way F_{F1} and F_{F2} are determined is by calculating a linear regression in the interval $[-1, 1]$ mm and then taking the value at mid-stroke. As explained in section 4.3, between two strokes ($\pm$ 10 mm)

a delay of 2 sec is added. This enables the determination of the static friction. The calculation of the static friction is analogous to the calculation of the sliding friction and is given in (13) and (14).

$$F_{stat_{exten}} = F_{F3} - F_{F4} \tag{13}$$

$$F_{stat_{comp}} = F_{F5} - F_{F6} \tag{14}$$

Determining the friction force components (F_{F3} to F_{F6}) is done differently. In a 1 mm interval at the end (or beginning) of the stroke the maximum (or minimum) force is taken as the friction force component. Figure 19 shows graphically how F_{F3}, F_{F4}, F_{F5} and F_{F6} are determined.

The gas force at mid-stroke is calculated by taking the average of F_{F1} and F_{F2} (15). The gas force is proportional to the gas pressure, and the gas pressure is proportional the volume of rod entering the working chamber (7). Therefore, the gas force varies linearly with the axial displacement. By taking the average of the linear regressions that are used to determine F_{F1} and F_{F2}, the linear relation of the gas force is obtained (dashed line in figure 19).

$$F_{gas} = \frac{1}{2}\left(F_{F1} + F_{F2}\right) \tag{15}$$

Two shock absorbers have been tested, shock absorber 1 is of the twintube type while shock absorber 2 is a monotube shock absorber. The friction and gas test results of both shock absorbers is shown in figures 20 and 21. The graph shows the six friction force components that are used to calculate the friction and gas forces. The resulting friction and gas forces are summarised in table 4. Note that the gas force is negative as this is a jounce force. Comparing the actual measurement of figure 21 with the schematic shown in figure 19, it can be seen that the there is no peak present at F_{F5}. This is explained by the fact that the magnitude of the gas force overcomes the static friction. As explained before, the gas force is a jounce force, aiding the extension of the shock absorber and therefore also influencing the friction. The gas force effectively increases the static friction at extension and reduces the static friction at compression.

Table 4: Friction and gas forces for both measured shock absorbers

	F_{gas} [N]	F_{slide} [N]	$F_{stat_{exten}}$ [N]	$F_{stat_{comp}}$ [N]
Shock absorber 1 (twintube)	-95	90	102	89
Shock absorber 2 (monotube)	-176	29	41	26

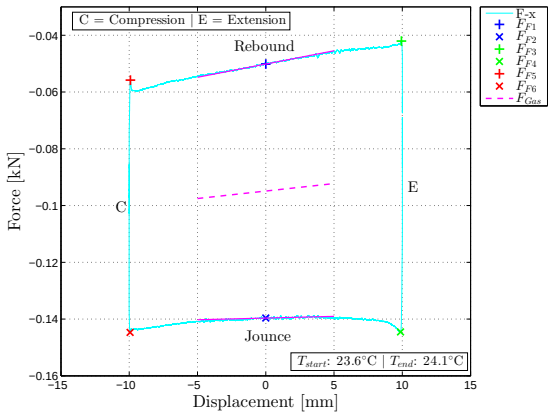

Figure 20: Friction and gas test for the twintube shock absorber

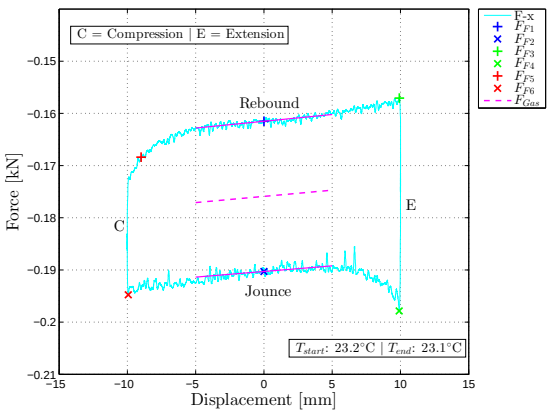

Figure 21: Friction and gas test for the monotube shock absorber

A small final note can be made about the temperature at the end of the friction and gas test in figure 20. Namely, it is higher than at the start. This can have two reasons:

1. The ambient temperature was higher than the starting temperature.
2. or, the shock absorber was cold, requiring the warm-up sequence to run for a significant amount of time. If the cycle takes longer to warm up, it takes longer for the temperature to settle. The automated test procedure is unable to wait for the temperature to settle.

5.2 Work Diagram

One way to show the shock absorber characteristics as a result of the VDA standard + high speed test is the work diagram. The work diagram, commonly known as the "Potato"-graph, visualises the force versus displacement characteristics. As pointed out in section 4.4, the third cycle for each sinusoid is extracted. The work diagram shows the force versus displacement data of this cycle for each individual speed. The rebound strokes are shown at the top half of the graph (force positive), the jounce strokes are shown on the bottom half (force negative). Figure 22 and 23 show the work diagram of both measured shock absorbers introduced in section 5.1. Apart from the larger amplitude at maximum stroke velocity, which is a performance related problem (see section 5.4), one can see that for stroke velocities higher than 1047 mm/s there is a delay in force built up going from rebound to jounce. This attributes to the cavitation effect that has been explained in section 2.2. There could be multiple reasons that could cause this effect. The most probable explanation is a combination of:

1. too low gas pressure
2. tight restriction around the base valve
3. tight restriction around the piston

Shock absorber 2 on the other hand shows a very normal work diagram up to a stroke velocity of 2000 mm/s. The two largest stroke velocities show a force built up at the end of the jounce stroke even though the stroke velocity is already decreasing. This is attributed to the complex combination of gas pressure and piston valve design.

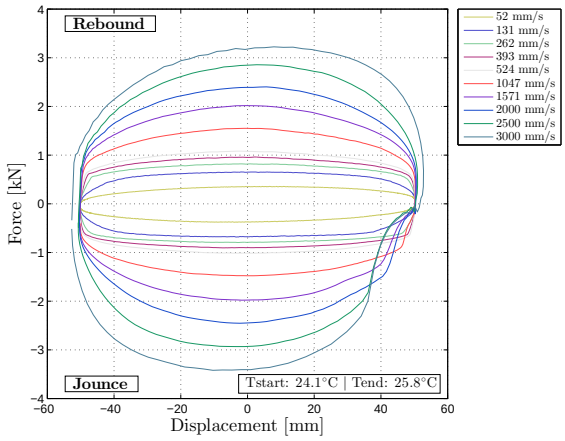

Figure 22: Work diagram for the twintube shock absorber

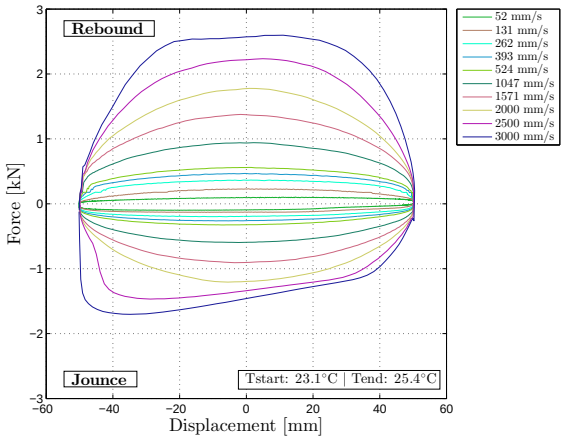

Figure 23: Work diagram for the monotube shock absorber

5.3 Characteristic Diagram

The characteristic diagram is used to investigate the damping force generation for the ten different stroke velocities from table 3. There are two types of characteristic diagrams:

1. force versus velocity: this diagram gives insight into how the force is generated as a result of the sinusoidal velocity input. More importantly, one can gain insight into the hysteresis characteristics of the shock absorber. Hysteresis captures the directionality characteristics of an input. A shock absorber generates different damping forces at identical stroke velocities in a rebound stroke compared to a jounce stroke. This hysteresis effect is the largest at low speeds represented schematically by "Main Hysteresis Loop" in figure 24. There are also smaller differences when building up the maximum stroke velocity compared to slowing down from this maximum velocity. This hysteresis effect is represented by "Small Hysteresis" in figure 24.

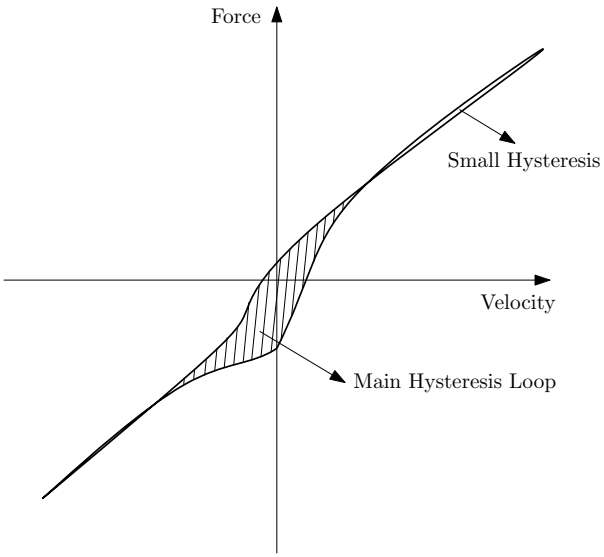

Figure 24: Hysteresis loop in a force-velocity graph

In real world, these hysteresis effects in shock absorbers can pose unwanted side effects on ride comfort. Due to the absence of good models that can incorporate these effects, tuning of dampers for ride comfort is still purely performed on a subjective basis as explained in section 2.4. The measurements are performed afterwards to complement the subjective findings. Figures 25 and 26 show the force-velocity diagrams for both of the measured shock absorbers. It can be seen that the cavitation effect in shock absorber 1 is a large contribution to the hysteresis effect. The force built up observed in the work diagram of shock absorber 2 also contributes to a large hysteresis effect.

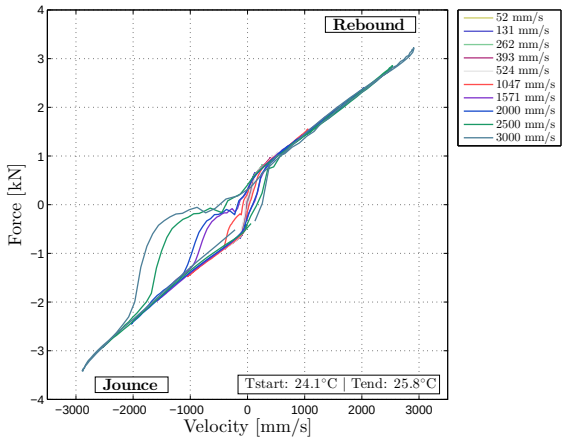

Figure 25: Characteristic diagram - force versus velocity for the twintube shock absorber

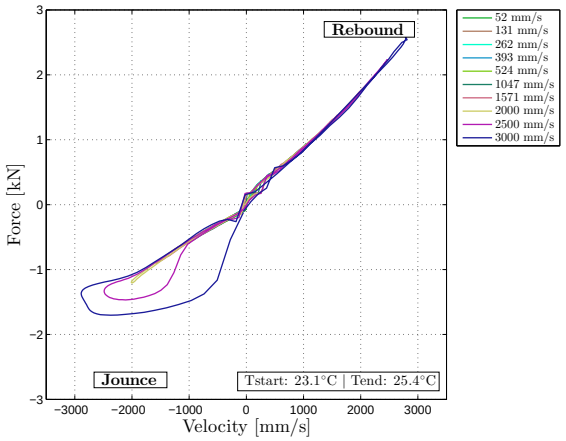

Figure 26: Characteristic diagram - force versus velocity for the monotube shock absorber

2. force at peak velocity: this graph shows the force at the peak rebound and peak jounce velocities and is given in figures 27 and 28. Note that jounce velocity is displayed as positive in this type of graph. Complementing this figure is a table with the actual values of the force and velocity, as an example the table for shock absorber 1 is shown in table 5. This table also shows the energy dissipated by the shock absorber during the entire cycle. The dissipated energy is calculated as the work performed by the shock absorber. This is done by summing the instantaneous force multiplied by the section of path it is acting on (16). This also corresponds to the contour integral of the work diagram.

$$W = \sum F_i \cdot (x_i - x_{i-1}) \tag{16}$$

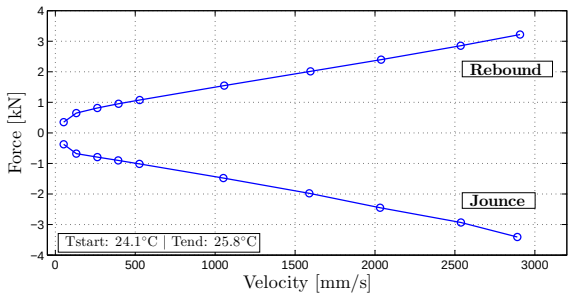

Figure 27: Characteristic diagram - force at peak velocity for the twintube shock absorber

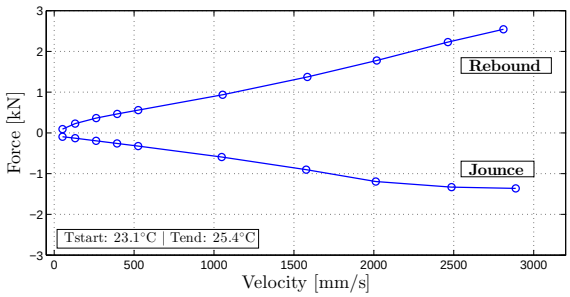

Figure 28: Characteristic diagram - force at peak velocity for the monotube shock absorber

Table 5: Shock absorber 1 performance overview

[mm/s]	Peak Rebound Velocity [mm/s]	Peak Rebound Force [N]	Peak Jounce Velocity [mm/s]	Peak Jounce Force [N]	Amplitude [mm]	Energy [kN mm]
52	52.1	351.6	52.1	-375.1	50.1	59.5
131	131.4	648.5	131.3	-676.8	50.1	115.4
262	262.9	815.8	262.5	-792.4	50.2	144.7
393	395.4	952.2	393.6	-900.5	50.2	166.0
524	527.6	1076.6	525.8	-1015.7	50.2	185.3
1047	1056.3	1549.6	1051.2	-1479.0	50.3	258.5
1571	1596.2	2014.1	1588.6	-1977.9	50.4	328.4
2000	2037.9	2397.3	2032.1	-2448.7	50.6	395.6
2500	2536.0	2852.3	2539.3	-2932.4	51.0	468.2
3000	2907.5	3217.2	2891.2	-3407.5	52.8	559.7

5.4 Rig Performance

To gain insight into how well the rig performed the test, a rig performance table is given out after each test (table 6). This table is closely related to table 5. It shows the peak rebound and jounce velocities with their deviation from the input together with the amplitude and the deviation in amplitude. This gives insight into how well the SAR is tuned. If deviations are too large one can choose to check the tuning of the machine. The report warns the operator if for a certain velocity the deviation in amplitude is larger than 2% or if the deviation in velocity is larger than 5%.

Table 6: Rig performance overview after testing shock absorber 1

	Peak Rebound Velocity	Velocity Deviation	Peak Jounce Velocity	Velocity Deviation	Amplitude	Amplitude Deviation
[mm/s]	[mm/s]	[%]	[mm/s]	[%]	[mm]	[%]
52	52.1	0.22	52.1	0.20	50.1	0.28
131	131.4	0.29	131.3	0.19	50.1	0.24
262	262.9	0.35	262.5	0.21	50.2	0.31
393	395.4	0.59	393.6	0.14	50.2	0.37
524	527.6	0.68	525.8	0.34	50.2	0.39
1047	1056.3	0.88	1051.2	0.40	50.3	0.62
1571	1596.2	1.61	1588.6	1.12	50.4	0.87
2000	2037.9	1.89	2032.1	1.61	50.6	1.22
2500	2536.0	1.44	2539.3	1.57	51.0	1.96
3000	2907.5	-3.08	2891.2	-3.63	52.8	5.55

6 Conclusion

During this internship a basic knowledge has been attained of automotive shock absorbers used today. The basic operating principles of the monotube and twintube hydraulic shock absorbers have been set forth and the motions that are preferably damped out by them were listed. Unfortunately, there is always a big trade-off between performance (safety) and comfort. To get the optimum damping performance to damp out these motions shock absorbers are tuned by changing the valve configuration. After a certain valve configuration is chosen it can be tested in a shock absorber rig. This report covered a short overview of the updated servo-hydraulic SAR at LPG and the tuning procedure to get the optimum performance for a shock absorber test.

A shock absorber measurement procedure has been configured consisting of a lock check, temperature check, friction and gas test and VDA standard + high speed test. The actual measurements to characterise the shock absorber are taken in the latter two parts of the procedure. The friction and gas test consists of a rebound and jounce stroke between ± 10 mm at a very low stroke velocity of 0.4 mm/s. The result from this test is the gas force at mid-stroke, the static friction at extension ($+10$ mm) and compression (-10 mm), and the sliding friction at mid-stroke. The VDA standard + high speed test consists of a series of sines with an amplitude of 50 mm and 10 stroke velocities. The results of these measurements can be expressed in several ways through either work or characteristic diagrams or by displaying the results in a tabular form. As became clear during the discussion of actual test results, side-effects such as cavitation can be recognised and hysteresis properties can be quantified. Together, the friction and gas test and the VDA standard + high speed test give a good overview of the main characteristics of the shock absorber that was tested.

As a final note it can be said that the measurement procedure with the Ford LPG shock absorber rig has been enhanced. An easy to use post-processing tool has been developed and a clear overview of the results of the measurements is given in a five page report.

6.1 Recommendations

To be able to enhance the quality of the measurements even further, the tuning of the rig could be performed more rigorously using a frequency response function (FRF) measurement of the rig. Using this FRF measurement all eigenmodes of the system can be identified and the performance of the rig can be analysed which can be used to determine the tuning parameters.

The measurement procedure can also be improved. At this point only one amplitude and a discrete sequence of 10 sines are considered. However, it would be interesting to investigate the behaviour of the shock absorber for a broader spectrum of sines and larger set of amplitudes because the shock absorber is a nonlinear system.

References

[1] S. Cafferty and G. Tomlinson. Characterization of automotive dampers using higher order frequency response functions. Paper, University of Sheffield, Department of Mechanical Engineering, 1997.

[2] MTS Systems Corporation. Model 793.00 system software. System Manual, 2003.

[3] J. Dixon. *The Shock Absorber Handbook*. John Wiley and Sons, Ltd., 2007.

[4] P. Els, N. Theron, P. Uys, and M. Thoresson. The ride comfort vs. handling compromise for off-road vehicles. Paper, University of Pretoria, Department of Mechanical Engineering and Aeronautical Engineering, 2007.

[5] T. Gillespie. *Fundamentals of Vehicle Dynamics*. Society of Automotive Engineers, Inc., 1992.

[6] A. Lordick and J. Watson. Shockabsorber ces. Ford Motor Company Core Engineering Specification, 2014.

[7] U. Neureder. Spring aid dynamic characterisation. Ford Motor Company Test Procedure, 2008.

[8] U. Neureder. What dampers should do and what they actually do. Ford Motor Company Training, 2008.

[9] U. Neureder. Ride comfort fundamentals. Ford Motor Company Training, 2011.

[10] International Organisation of Standardization. Mechanical vibration and shock - evaluation of human exposure to whole body vibration. ISO 2631-1 second edition, 1997.

[11] BASF Polyurethanes. Cellasto spring aids. http://www.polyurethanes.basf.de/pu/Cellasto/Die_Zusatzfeder/Die_Zusatzfeder-Eine_saubere_Sache. Accessed December 7, 2016.

[12] J. Watson. Shock absorber training. Ford Motor Company Training, 2005.

Appendix A Reports

The following pages contain the standardised reports that are automatically generated using the graphical user interface (GUI) designed during this internship. The GUI was designed such that the mechanics at LPG, who only have a very basic knowledge of MATLAB, could easily run the post-processing and generate reports. The lay-out of this GUI is shown in figure 29.

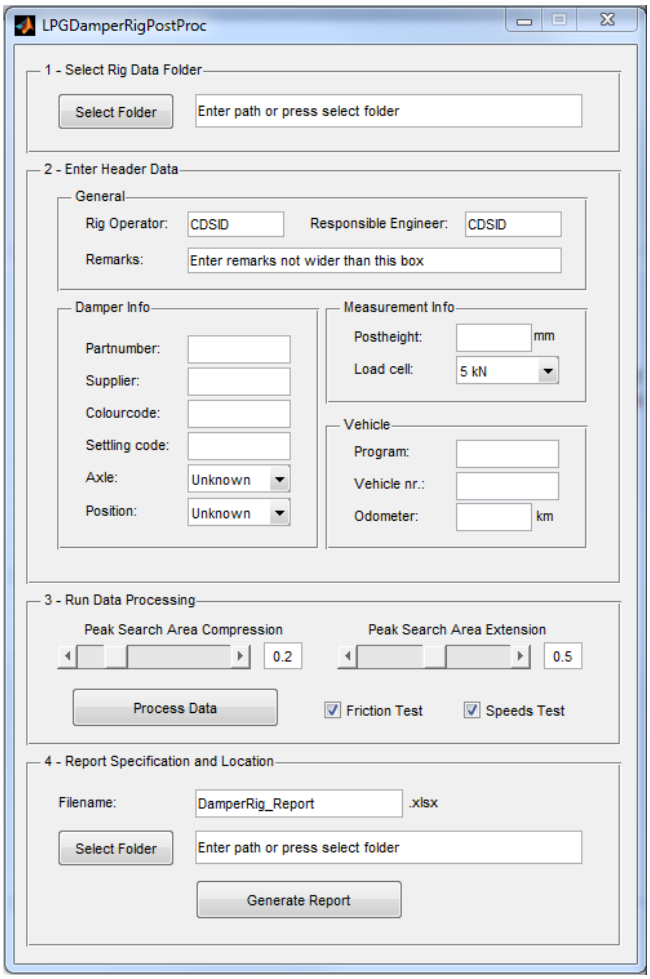

Figure 29: Graphical user interface to run the MATLAB post-processing scripts

GlobalVehicleDynamics

VD Methods and Tools
Lommel Proving Ground

Friction and Gas Test − 20161202_DampertestReport_1

Operator: *tdemoree* Engineer: *rhendri9* Test Executed: *02/12/2016 12:19:44*

Remarks:

Measurement Info

Rig:	*VehDyn*	Stroke:	*20 mm*	Postheight:		**Vehicle**	
Method:	*EngSpec*	Gas Cor.:	*Yes*	Load Cell:	*5 kN*	Program:	
						Vehicle Nr:	
						Odo−meter:	

Damper

Partnr.:	Supplier:	Colorcode:		
Settling:	Axle:	Position:		

Damper Losses

Gas Force:	*−95 N*	Sliding Fric.:	*90 N*	Static Fric. E:	*102 N*	Static Fric. C:	*89 N*

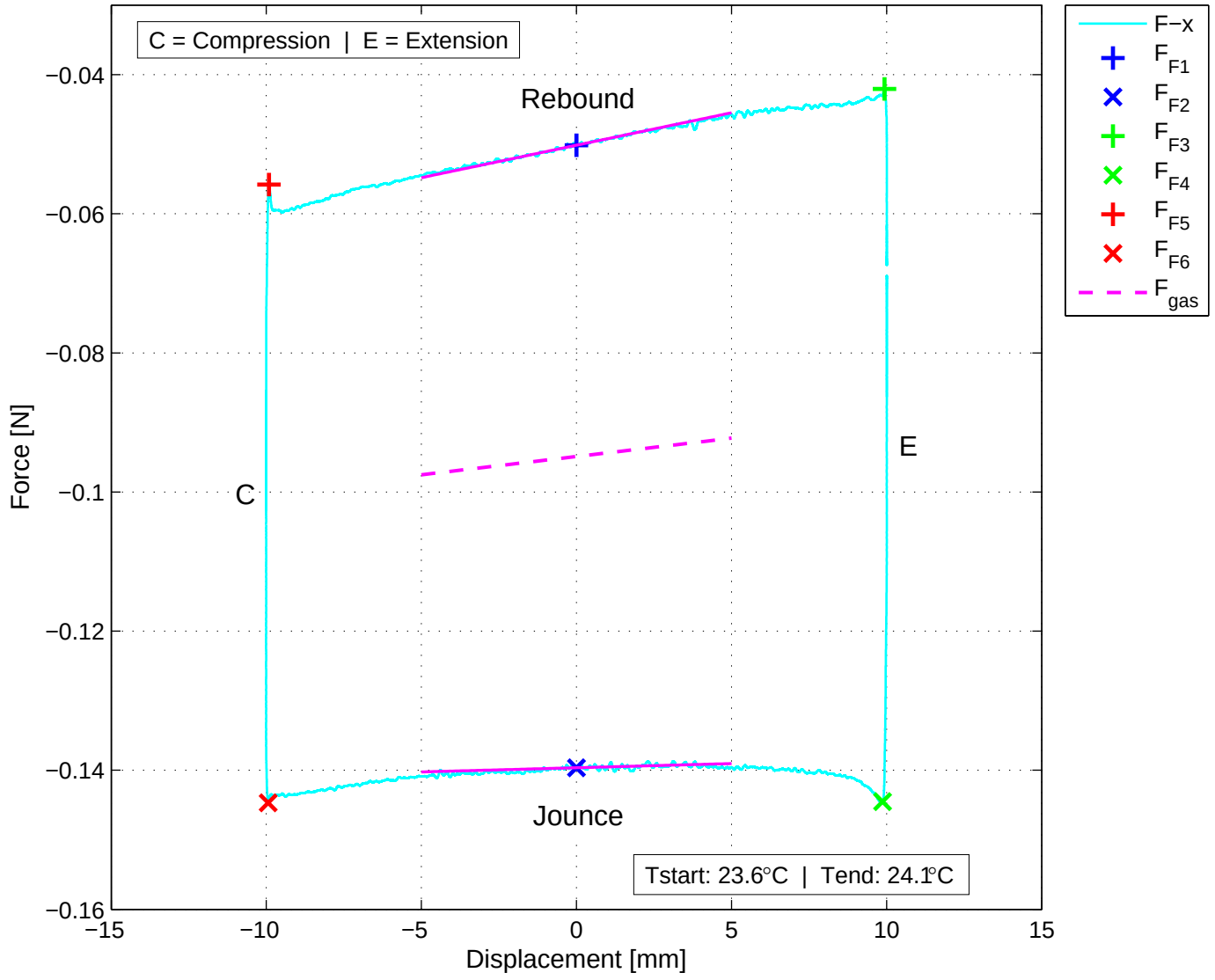

Friction and Gas Forces

F_{F1}:	*−50 N*	F_{F3}:	*−42 N*	F_{F5}:	*−56 N*
F_{F2}:	*−140 N*	F_{F4}:	*−145 N*	F_{F6}:	*−145 N*

GlobalVehicleDynamics

VD Methods and Tools
Lommel Proving Ground

VDA Force vs. Displacement − 20161202_DampertestReport_1

Operator: *tdemoree* Engineer: *rhendri9* Test Executed: *02/12/2016 12:21:34*

Remarks:

Measurement Info

Rig:	*VehDyn*	Stroke:	*100 mm*	Postheight:		**Vehicle**	
Method:	*VDA*	Gas Cor.:	*Yes*	Load Cell:	*5 kN*	Program:	
						Vehicle Nr:	
						Odo−meter:	

Damper

Partnr.:	Supplier:	Colorcode:		
Settling:	Axle:	Position:		

Damper Losses

Gas Force:	*−95 N*	Sliding Fric.:	*90 N*	Static Fric. E:	*102 N*	Static Fric. C:	*89 N*

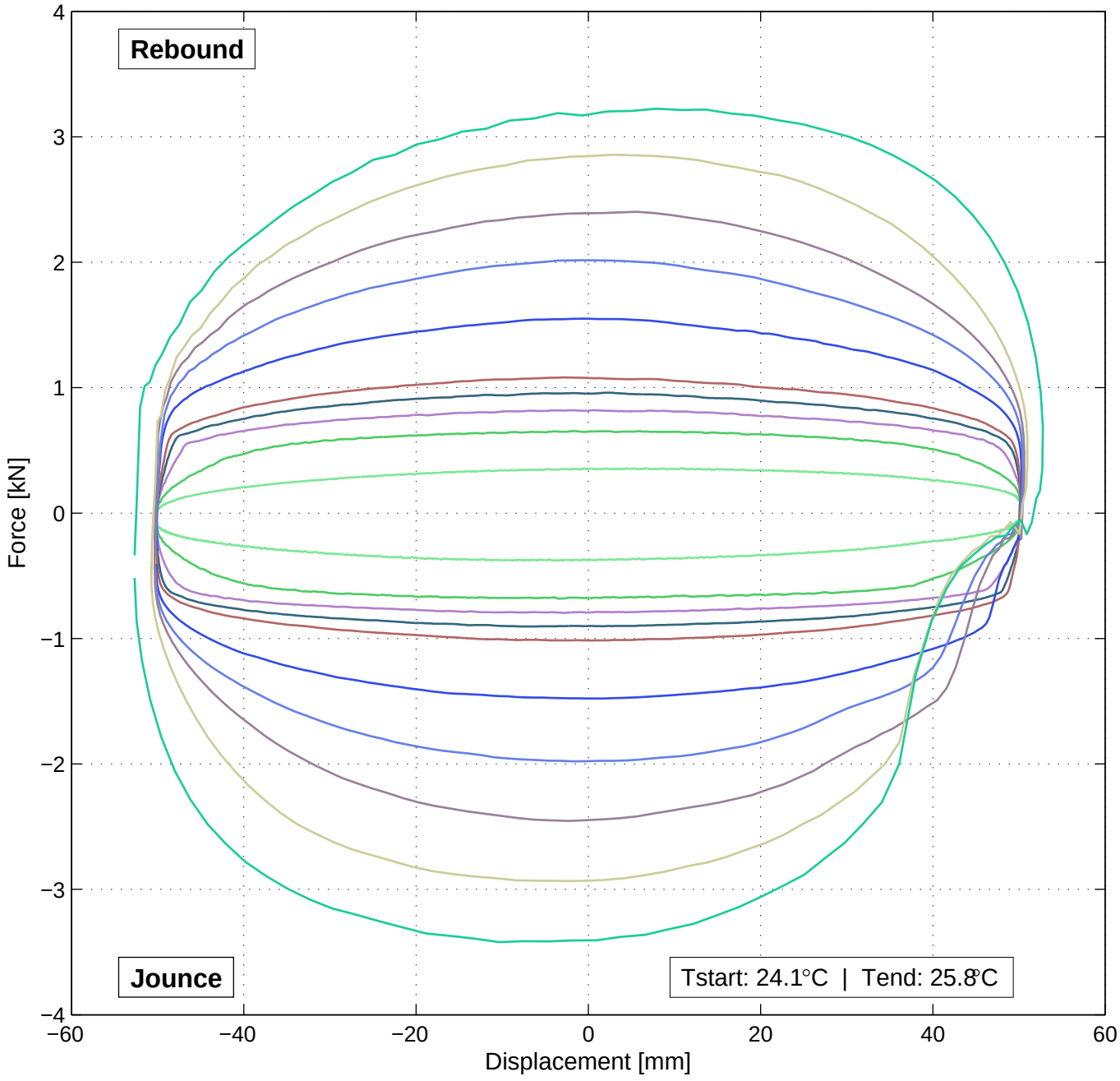

GlobalVehicleDynamics

VD Methods and Tools
Lommel Proving Ground

VDA Force vs. Velocity − 20161202_DampertestReport_1

Operator: *tdemoree* Engineer: *rhendri9* Test Executed: *02/12/2016 12:21:34*

Remarks:

Measurement Info

Rig:	*VehDyn*	Stroke:	*100 mm*	Postheight:		**Vehicle**	
Method:	*VDA*	Gas Cor.:	*Yes*	Load Cell:	*5 kN*	Program:	
						Vehicle Nr:	
						Odo−meter:	

Damper

Partnr.:	Supplier:	Colorcode:		
Settling:	Axle:	Position:		

Damper Losses

Gas Force:	*−95 N*	Sliding Fric.:	*90 N*	Static Fric. E:	*102 N*	Static Fric. C:	*89 N*

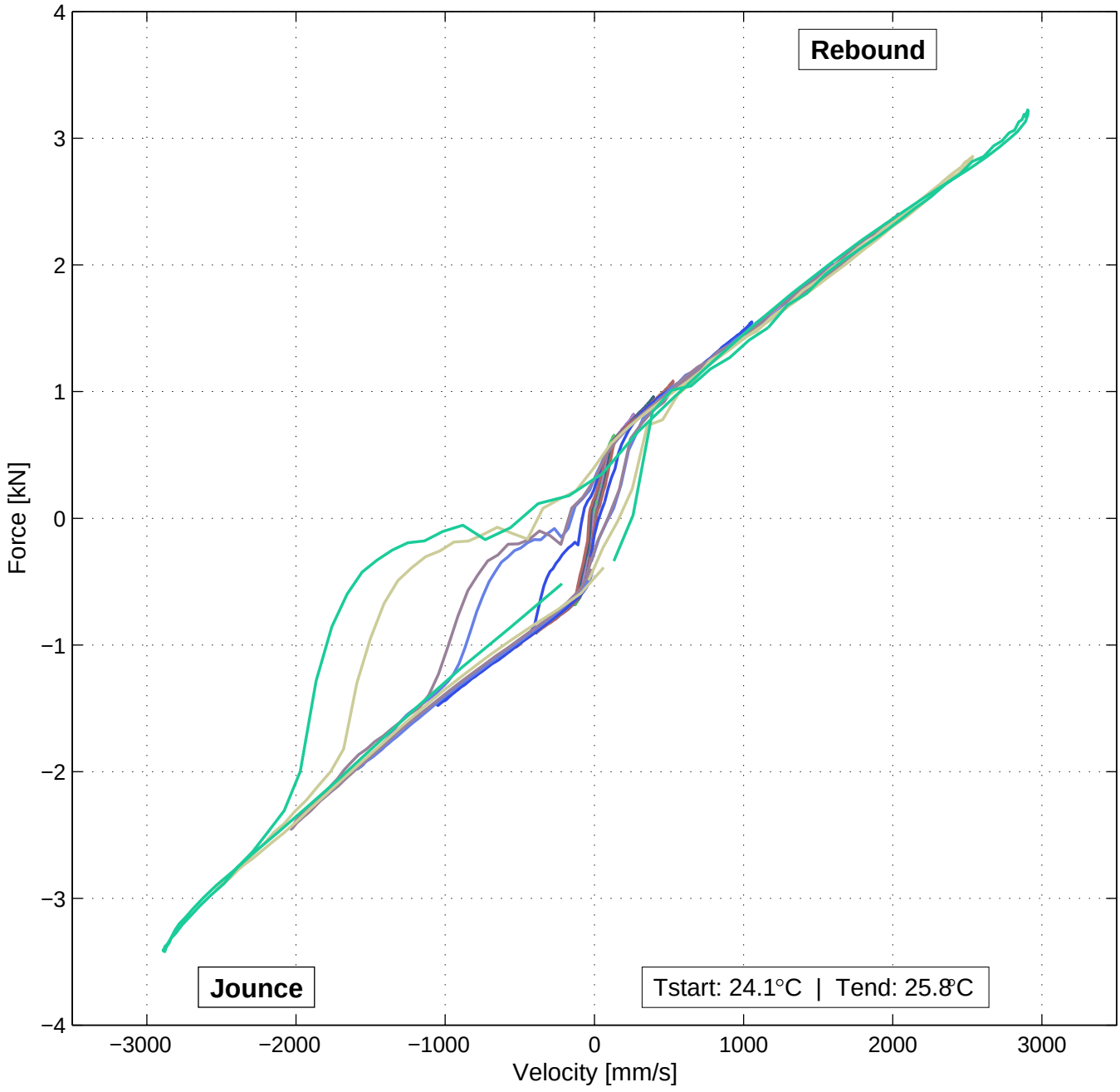

GlobalVehicleDynamics

VD Methods and Tools
Lommel Proving Ground

VDA Force vs. Peak Velocity − 20161202_DampertestReport_1

Operator: *tdemoree* Engineer: *rhendri9* Test Executed: *02/12/2016 12:21:34*

Remarks:

Measurement Info

Rig:	*VehDyn*	Stroke:	*100 mm*	Postheight:		**Vehicle**	
Method:	*VDA*	Gas Cor.:	*Yes*	Load Cell:	*5 kN*	Program:	
						Vehicle Nr:	
						Odo−meter:	

Damper

Partnr.:	Supplier:	Colorcode:		
Settling:	Axle:	Position:		

Damper Losses

Gas Force:	*−95 N*	Sliding Fric.:	*90 N*	Static Fric. E:	*102 N*	Static Fric. C:	*89 N*

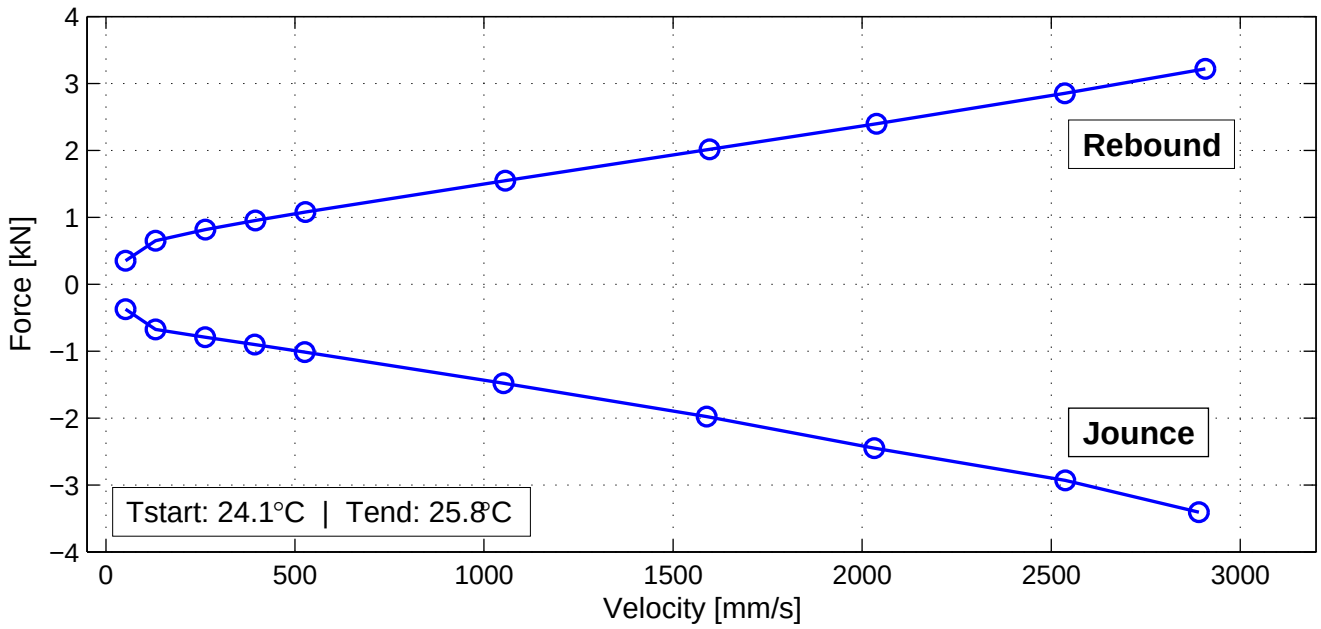

	Peak Rebound Velocity	Peak Rebound Force	Peak Jounce Velocity	Peak Jounce Force	Amplitude	Energy
[mm/s]	[mm/s]	[N]	[mm/s]	[N]	[mm]	[kN mm]
52	52.1	351.5	52.1	−374.5	50.1	59.5
131	131.4	648.5	131.3	−677.5	50.1	115.4
262	262.9	815.8	262.5	−792.4	50.2	144.7
393	395.3	952.2	393.6	−900.5	50.2	166.0
524	527.6	1076.6	525.9	−1015.7	50.2	185.3
1047	1056.3	1546.6	1051.2	−1479.0	50.3	258.5
1571	1596.4	2014.1	1588.6	−1977.9	50.4	328.4
2000	2038.1	2397.3	2032.1	−2448.7	50.6	395.6
2500	2536.1	2852.3	2537.4	−2932.4	51.0	468.2
3000	2907.5	3217.2	2890.3	−3407.5	52.8	559.7

GlobalVehicleDynamics

VD Methods and Tools
Lommel Proving Ground

VDA Machine Performance − 20161202_DampertestReport_1

Operator: *tdemoree* Engineer: *rhendri9* Test Executed: *02/12/2016 12:21:34*

Remarks:

Measurement Info

Rig:	*VehDyn*	Stroke:	*100 mm*	Postheight:		**Vehicle**	
Method:	*VDA*	Gas Cor.:	*Yes*	Load Cell:	*5 kN*	Program:	
						Vehicle Nr:	
						Odo−meter:	

Damper

Partnr.:	Supplier:	Colorcode:		
Settling:	Axle:	Position:		

Damper Losses

Gas Force:	*−95 N*	Sliding Fric.:	*90 N*	Static Fric. E:	*102 N*	Static Fric. C:	*89 N*

Damper Rig Performance Metrics:

To check how well the damper rig performs the test, the normalized deviation in amplitude and stroke velocity is calculated. The velocity is allowed to deviate 5% and the amplitude 2%.

	Peak Rebound Velocity	Rebound Vel. Deviation	Peak Jounce Velocity	Jounce Vel. Deviation	Amplitude	Amplitude Deviation
[mm/s]	**[mm/s]**	**[%]**	**[mm/s]**	**[%]**	**[mm]**	**[%]**
52	52.1	0.22	52.1	0.20	50.1	0.28
131	131.4	0.29	131.3	0.19	50.1	0.24
262	262.9	0.35	262.5	0.21	50.2	0.31
393	395.3	0.58	393.6	0.14	50.2	0.37
524	527.6	0.69	525.9	0.36	50.2	0.39
1047	1056.3	0.89	1051.2	0.40	50.3	0.62
1571	1596.4	1.62	1588.6	1.12	50.4	0.87
2000	2038.1	1.91	2032.1	1.60	50.6	1.22
2500	2536.1	1.44	2537.4	1.49	51.0	1.96
3000	2907.5	−3.08	2890.3	−3.66	52.8	5.55

Appendix B Spring Aid Dynamic Characterisation

Although the main purpose of the LPG SAR is to test shock absorbers, there are also other applications that could be considered. During my internship, I was therefore asked to also explore the possibility of testing spring aids. Spring aids are progressive bump stops that are placed either on the rod of the shock absorber or inside a coil or pneumatic spring. Many other applications of the spring aid are possible. An example of spring aids that are put on the piston rod of a shock absorber is shown in figure 30. In most automotive applications, they are used to progressively ease into the end of the suspension travel. This makes reaching the end of the suspension travel more comfortable by avoiding metal-to-metal contact and prevent destruction.

Figure 30: BASF Cellasto spring aid for placement on piston rod of a shock absorber [11]

The purpose of this test is to characterise the dynamic properties of a spring aid. During this test, the spring aid is compressed up to 85% of its full compression amplitude by a 1 Hz sinewave. Half of the cycle of the sinewave travels through free air while the other half compresses the spring aid. The test is executed for five cycles (5 sec) [7].

Figure 31 shows the force built up with time. It can be seen that the first two force peaks are higher than the average of the following three peaks. Due to the material properties of the spring aid, the initial stiffness is slightly higher. To gain insight into the stiffness of the spring aid, figure 32 is created. This figure shows the stiffness versus deflection to see how the stiffness varies as the spring aid is compressed.

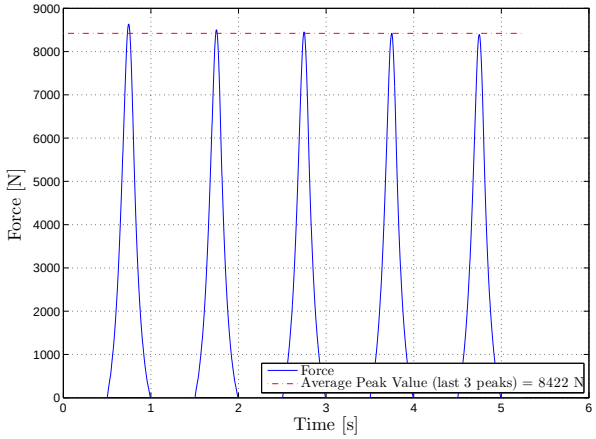

Figure 31: Spring aid peak force

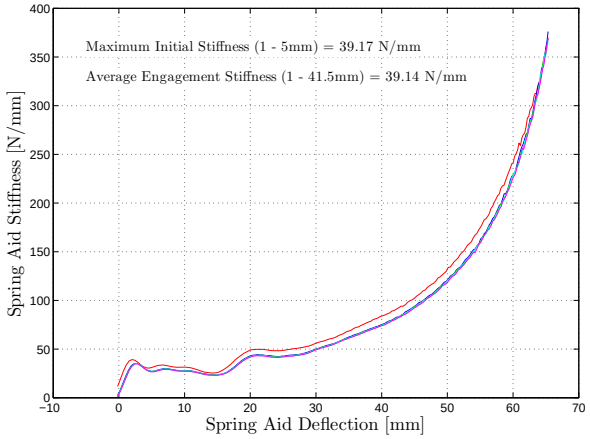

Figure 32: Spring aid stiffness

Appendix C 4-Poster for Ride Comfort Measurements

LPG is equipped with a 4-poster testing facility. This essentially allows the car to be put on four "posts" which can actuate each wheel individually to play a certain road profile. Usually, this machine is used for NVH (Noise, Vibration and Harshness) tests to determine annoying squeaks and rattles that can negatively influence customer satisfaction. The road profile that is used for NVH tests consists of a series of noise inputs to shake the car. However, the ride comfort of the car can also be measured using the 4-poster. This is done by using a specialised camera system combined with strategically placed accelerometers. The road profile that is used are the actual ride and comfort tracks at LPG. Benefits of using the 4-poster testing facilities are:

1. The road profile is exactly the same for each test and each vehicle. When performing a ride measurement on the actual ride and comfort tracks it is important to drive exactly in the middle of the lane to have a comparable road profile to compare results between different tests and vehicles. In other words, there is a huge dependency on the driver performing the test.
2. Vehicle motions can be measured from outside the vehicle. When performing real-life ride measurements, all sensors are placed on the car. With the 4-poster, the motions of the car can be captured using a camera system or optical measurement system (OMS) that is placed independently.
3. Controlled climate

During this internship, I was involved with a problem with the OMS. The OMS measures the xyz-displacement of predefined markers. One marker is placed on the wheel, and one marker on the body. The system has a set of limitations within which it can accurately perform the measurements. Firstly it has an operating window of 420 by 360 mm, and secondly, the distance of the camera to the marker should be 730 mm ($\pm$ 2 mm) to measure at peak accuracy. When during the measurements, one marker is not detected for a certain amount of seconds the post-processing programme fails to process the data. A second problem that was found is that sometimes during a limited amount of time a marker is lost. This usually happens at peaks of displacement which are mostly the peaks that needed to be examined.

The task at hand was firstly to come up with a certain road test profile that can be used to check the detection of the markers. And secondly, to create a programme which can easily visualise the position of the markers within the field of view of the camera such that the camera's can be positioned correctly for the actual test.

C.1 Road Test Profile

The road profile to test the OMS should meet the following requirements:

1. it should be challenging such that the limits of the OMS can be found.
2. it should be a relatively short test such that the limits can be quickly detected and the post-processing of the images does not take too long.

To meet the requirements, three sections were selected. A 60 sec section of the most demanding ride road at LPG has been taken. Next, a demanding speed bump followed by a ramp up and down to 90% of the displacement limits of the 4-poster. The lay-out of this road profile is shown in figure 33. It can be seen that it has a track for the wheels on the left side of the car, and a track for the right side of the car. Next, there is also a distinction between front and rear. This is a delay that is added to the system based on the length of the wheelbase and the speed that is travelled over the bumps. The speed is 60 km/h and with a wheelbase of 2680 mm this results in a delay of 159 msec.

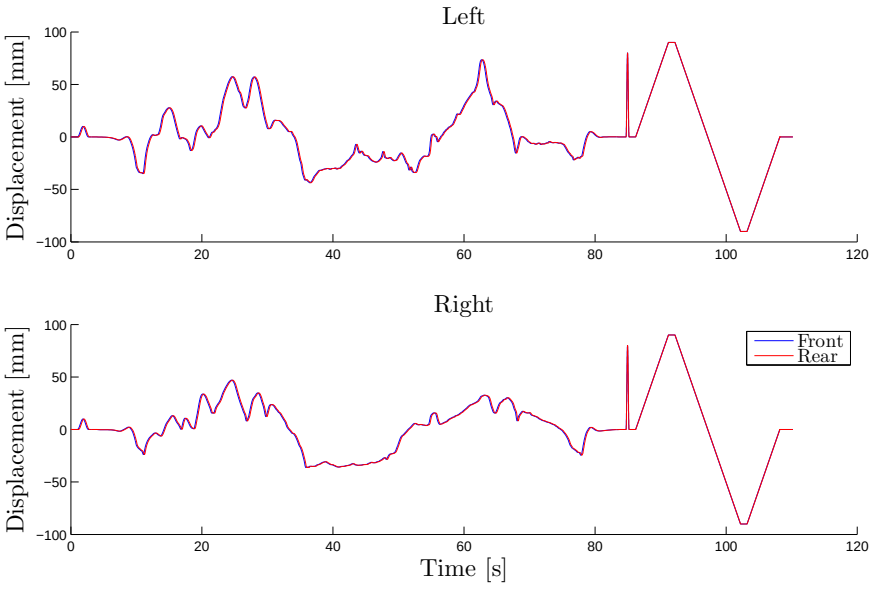

Figure 33: Road test profile for a vehicle with a wheelbase of 2650 mm

C.2 Camera Check

After the test is executed using the road profile discussed above, the images are processed by the OMS. The result of the post processing is a .csv file with the xyz-displacement of each marker at each wheel. Next, the camera check GUI is introduced. This GUI consists of two basic screens, one contains a lay-out with the displacement over time for each direction (see figure 34) and the other lay-out contains information about the effective field-of-view (fov) of the camera and the distance of the camera to the marker (see figure 36). Note that, the road profile has not been tested yet which means the data shown in the figures below is from one of the actual tests.

The first lay-out can be used to quickly check for abnormalities in the data set. As introduced above, it happens quite often that the peak displacement data fails to be recorded. Two examples of these abnormalities are given in figure 35. When these abnormalities are spotted, the reason for these abnormalities to occur can be found with the second lay-out. Figure 36 shows the second lay-out corresponding to the abnormalities (namely the left front wheel). It can be seen that the markers are within the field of view in the xy-direction. However, the camera at the left front wheel is placed too close to the body sticker. Placing the camera further away from the body is the only solution, but this causes the wheel (Rad) sticker to move further away as well. A solution could therefore be to glue a spacer (for instance a piece of foam) between the marker and the wheel to bring the marker in the same plane as the body.

The GUI is therefore a quick and easy tool to check the position of all four cameras and the displacement data of all the markers.

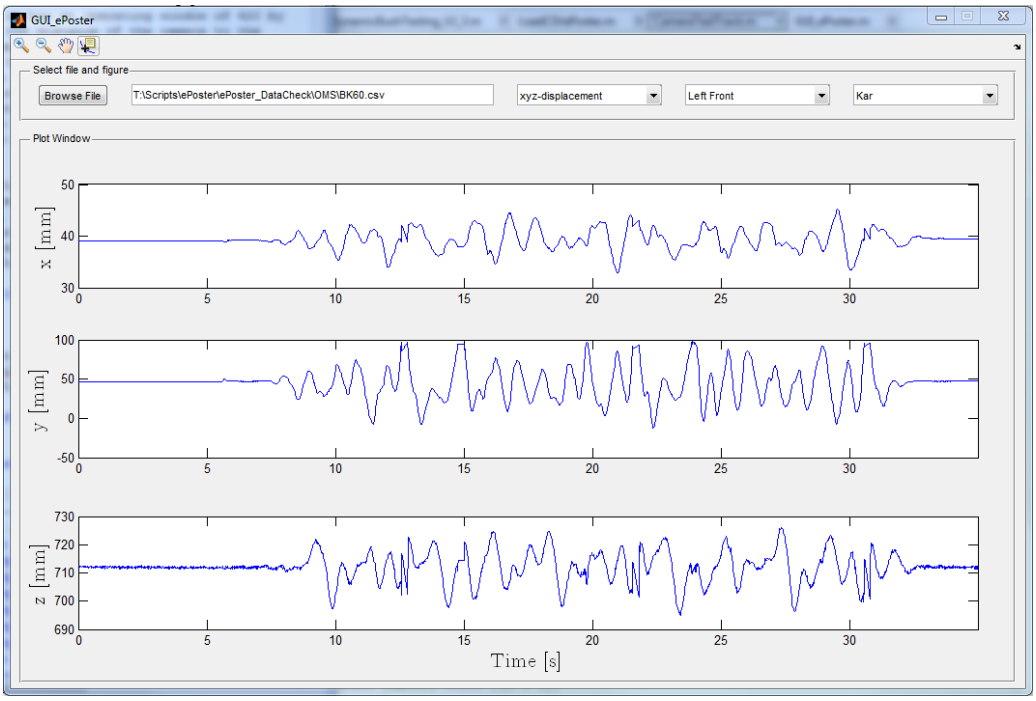

Figure 34: ePoster xyz-marker displacement checker

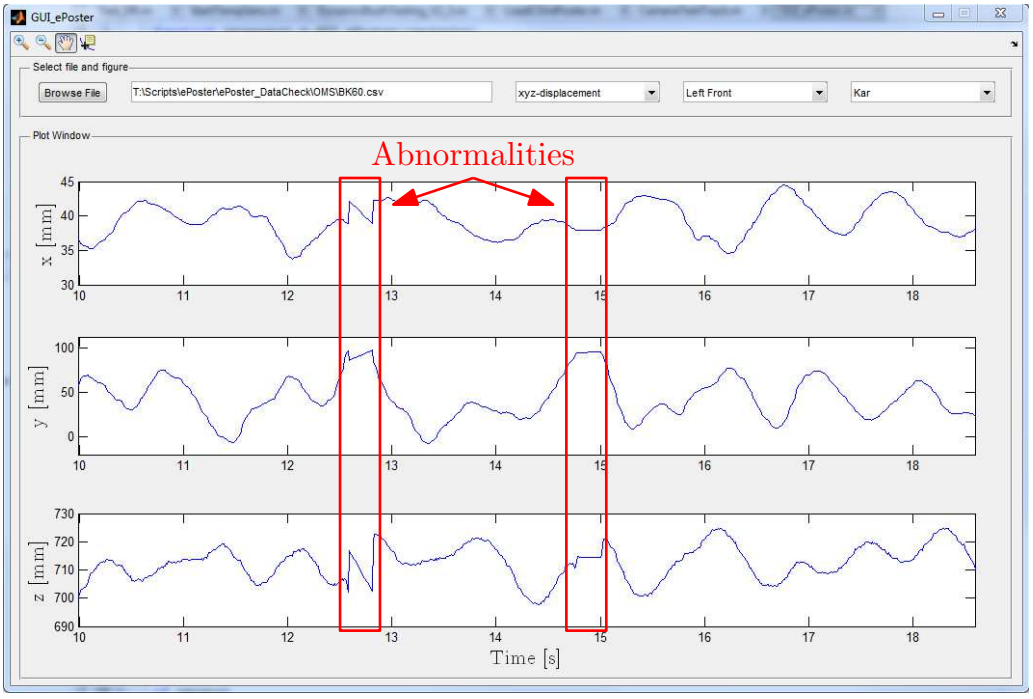

Figure 35: Abnormalities ePoster

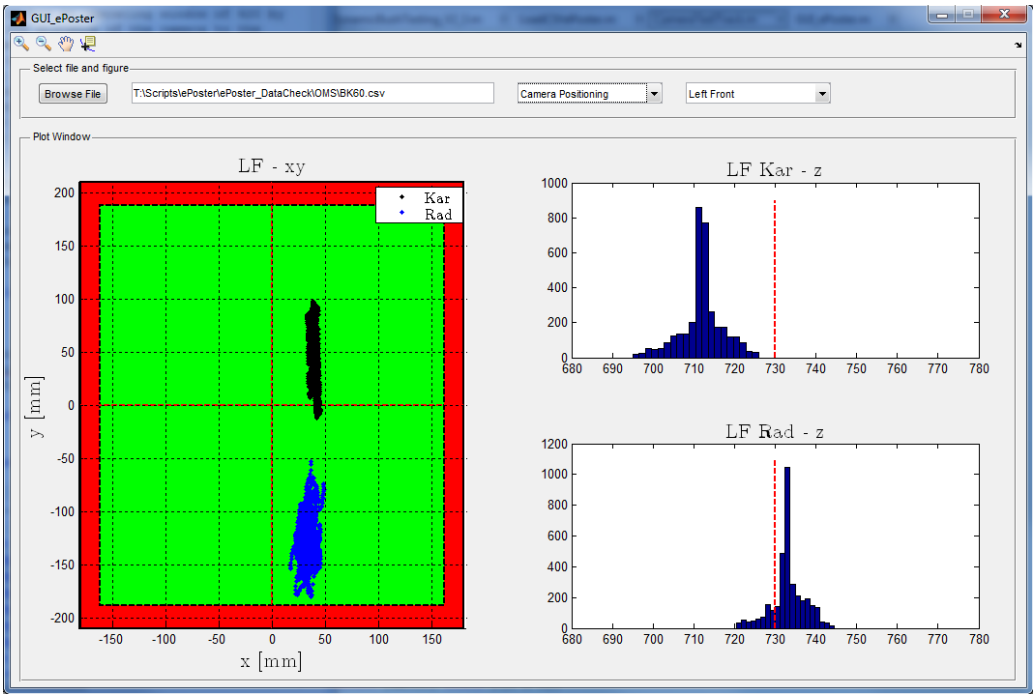

Figure 36: ePoster camera field of view and distance to marker checker